

CP violation in charged Higgs production and decays in the Complex Two Higgs Doublet Model

A. Arhrib^{a,b} E. Christova^c H. Eberl^d E. Ginina^{d,e}

^a*Département de Mathématique, Faculté des Sciences et Techniques, Université Abdelmalek Essaâdi, B. 416, Tangier, Morocco*

^b*LPHEA, Faculté des Sciences-Semlalia, B.P. 2390 Marrakesh, Morocco*

^c*Institute for Nuclear Research and Nuclear Energy, BAS, Sofia 1784, Bulgaria*

^d*Institut für Hochenergiephysik der Österreichischen Akademie der Wissenschaften, A-1050 Vienna, Austria*

^e*Universität Wien, Fakultät für Physik, A-1090 Vienna, Austria*

E-mail: aarhrib@ictp.it, echristo@inrne.bas.bg,
helmut@hephy.oeaw.ac.at, eginina@hephy.oeaw.ac.at

ABSTRACT: We study the effects of CP violation in charged Higgs boson production $pp \rightarrow tH^\pm + X$ at the LHC, as well as in the charged Higgs boson decays $H^\pm \rightarrow tb$ and $H^\pm \rightarrow W^\pm H_i^0$, $i = 1, 2, 3$. The study is done in the framework of the type II complex Two Higgs Doublet Model (2HDM) with softly broken Z_2 symmetry. In this model violation of CP invariance is induced by the complex parameter m_{12}^2 of the tree-level Higgs potential. We calculate the CP violating rate asymmetries for H^+ and H^- production and decays as well as for the combined processes at one-loop level and perform a detailed numerical analysis. All calculations are done with the automatic amplitude generator FeynArts and the calculational tool FormCalc, for which we have written a complete complex 2HDM model file and relevant fortran drivers. The implementation of the complex 2HDM in FeynArts and FormCalc is described. In comparison with the analogous results in the MSSM, all considered CP violating asymmetries are smaller by an order of magnitude and do not exceed $2 \div 3\%$.

KEYWORDS: Beyond Standard Model, CP-violation, Higgs Physics

ARXIV EPRINT: [1011.6560](https://arxiv.org/abs/1011.6560)

Contents

1	Introduction	2
2	General 2HDM: short review and notations	4
2.1	Scalar potential and its parameterization	4
2.1.1	Mass eigenstates	4
2.2	Z_2 symmetry and input parameter set	5
2.3	Higgs and gauge boson interactions	6
2.4	Yukawa interactions	7
2.5	Theoretical constraints on the Higgs potential	8
3	CP violation in H^\pm production and decays	8
3.1	The processes	8
3.2	CP violating asymmetries	9
3.3	CP violating loop contributions	10
4	Numerical results	13
4.1	Experimental constraints	13
4.2	CP violation in H^\pm -decays	14
4.3	CP violation in H^\pm -production	19
4.4	CP violation in H^\pm -production and subsequent decays	22
5	Conclusions	24
A	The $\Delta\rho$ constraint	24
B	Expressions for λ_i	25
C	Interaction Lagrangian	26
C.0.1	Interactions of two quarks with a gluon	26
C.0.2	Yukawa interactions of the neutral and the charged Higgses	27
C.0.3	Two quarks-W and two quarks-ghost interactions	27
C.0.4	Triple scalar interactions with neutral and charged Higgses	27
C.0.5	Neutral Higgs-charged Higgs-W and neutral Higgs-charged Higgs-ghost interactions	27
C.0.6	Interactions of a neutral Higgs with W-W, W-ghost and ghost-ghost	28
D	Implementation of the complex 2HDM into FeynArts and FormCalc	28
D.1	FeynArts model file for the C2HDM	28
D.2	FormCalc drivers for the C2HDM	29
D.2.1	Inputs	29
D.2.2	Constraints	30

1 Introduction

The CERN Large Hadron Collider (LHC) has started its operation aiming at a direct verification of one of the different candidates that generalize the Standard Model (SM). The experiments at the LHC have to distinguish between the predictions of the various theoretical models. Having in mind the large number of free parameters that most of these models introduce, this task is highly nontrivial. Powerful software and hardware resources are required so that their analyses lead to definite predictions for experimental searches.

An important approach for testing fundamental theories is studying discrete symmetries as model properties. In particular, the CP symmetry is known to be violated in nature [1–3]. According to Sakharov’s theorem, the mechanism of CP violation (CPV) in the SM is not strong enough to explain the baryon asymmetry in the universe – more CPV is needed. For that reason all models beyond the SM suggest additional and different sources of CPV.

On the other hand, the Higgs boson is not yet found and the mechanism of electroweak symmetry breaking (EWSB) remains the only part of the SM which is not yet verified. The extensions of the SM enlarge the Higgs sector and predict both charged and new neutral Higgs bosons. If a neutral Higgs boson is discovered at the LHC, there will be a long way to determine whether it belongs to the SM or to some of its extensions. A discovery of a charged Higgs boson though, would be a clear signal for Physics beyond the SM. A possibility to distinguish between the different models containing a charged Higgs is looking for effects of CPV in processes with H^\pm , which we shall explore in this paper.

The simplest extensions of the SM are the models with two Higgs doublets. All of them provide new sources of CPV. The most popular one is the Minimal Supersymmetric Standard Model (MSSM). The MSSM Higgs sector is a constrained 2HDM of type II. On the other hand, the general Complex Two Higgs Doublet Model (C2HDM) has attracted much attention due to the CPV it can accommodate [4–6] and due to its simplicity. The physical mass eigenstates in the Higgs sector of the 2HDM and the MSSM are the same – there are two charged H^\pm and three neutral H_i^0 , $i = 1, 2, 3$ Higgs bosons. Processes involving H^\pm can generate a CPV asymmetry at one-loop level in both MSSM and C2HDM. However, the CPV sources in these two models are different.

In the MSSM, the tree-level Higgs potential is real and thus the neutral Higgs bosons have definite CP parities and preserve CP invariance. CPV results from the non-zero CP phases of the higgsino mass parameter $\mu = |\mu| e^{i\phi_\mu}$ in the superpotential, the gaugino mass parameters $M_i = |M_i| e^{i\phi_i}$, $i = 1, 2, 3$, and the trilinear couplings $A_f = |A_f| e^{i\phi_f}$ (f stands for a fermion) in the soft SUSY breaking Lagrangian. In particular, in the MSSM neutral Higgs sector, the presence of these CP violating phases induces mixing between the CP-even and the CP-odd scalars at one-loop level, yielding three mass eigenstates [7].

In the C2HDM CPV is induced by the complex parameters of the tree-level Higgs potential and thus the physical neutral Higgs bosons are mixtures of the CP-even and the

CP-odd states. The interactions of these neutral Higgs bosons with fermions and gauge bosons violate CP invariance. We stress that in the C2HDM the mixture of the CP-even and the CP-odd neutral Higgs bosons is already at tree-level, while in the MSSM it is a loop-induced effect, generated by SUSY-loop corrections.

Effects of CPV in the decays of H^\pm into "ordinary" (SM) particles in the framework of the MSSM were studied in [8–11]. These CPV decay rate asymmetries are of interest for a future linear collider, where the charged Higgs will be produced in pairs. There CPV occurs only in the decays of H^\pm . For the LHC one must take into account CPV in the production process as well. Recently, $W^\pm H^\mp$ production at the LHC was studied in [12]. In [13–15] we studied CPV in the combined process of a charged Higgs boson production at the LHC:

$$pp \rightarrow H^\pm t + X, \quad (1.1)$$

followed by the subsequent decays of H^\pm , where the production process (1.1) is due to the partonic process $bg \rightarrow H^\pm t$. In both production and decays CPV is induced by one-loop radiative corrections with supersymmetric (SUSY) particles in the loops. Our numerical analysis showed that the CPV asymmetries, both in the decays and in the production, can be rather large. However, in the $H^\pm \rightarrow t\bar{b}$ decay mode, there can occur cancellations reducing the total asymmetry.

In this paper we perform an analogous study within the complex 2HDM. In addition to the production rate asymmetry we calculate the CPV decay rate asymmetries in the dominant decay modes of H^\pm in the C2HDM:

$$H^\pm \rightarrow tb \quad \text{and} \quad H^\pm \rightarrow W^\pm H_i^0, \quad i = 1, 2. \quad (1.2)$$

We also consider the CPV asymmetries in the combined processes of production (1.1) and decays (1.2). We work in type II C2HDM with softly broken Z_2 symmetry of the Lagrangian. In order to perform a numerical analysis, we have generalized the existing codes of the FeynArts (FA) and FormCalc (FC) packages [16–19], for calculating processes in the C2HDM.

The paper is organized as follows. In section 2 we shortly review the general 2HDM, fix the conventions for the scalar potential, the Yukawa interactions and the parameter set we work with. We derive the Higgs couplings to fermions and gauge bosons and list the existing theoretical constraints on the 2HDM Lagrangian. In the third section we study the production and decay processes mentioned above, present the expressions for the CPV asymmetries, and show the one-loop contributions to these asymmetries in the C2HDM. We proceed with a detailed numerical analysis in section 4. The numerical results for the CPV asymmetries in the charged Higgs decays (1.2), in the charged Higgs production (1.1), as well as for the combined process of production (1.1) and subsequent decays (1.2) at LHC at the center-of-mass energy $\sqrt{s} = 14$ TeV in the C2HDM are presented. We also discuss the experimental constraints on the C2HDM parameter space. The numerical analysis is done using the FA and FC packages. The implementation of the C2HDM into these packages is given in detail in the appendix, which also contains the Lagrangian relevant for

our study, the expression for $\Delta\rho$ implemented in the code and some important relations between the parameters of the scalar potential and the physical Higgs masses. As usual, the paper ends with conclusions.

2 General 2HDM: short review and notations

2.1 Scalar potential and its parameterization

The general 2HDM is obtained via extending the SM Higgs sector, consisting of one complex $Y=+1$, $SU(2)_L$ doublet scalar field Φ_1 , with an additional complex $Y=+1$, $SU(2)_L$ doublet scalar field Φ_2 . Using $\Phi_{1,2}$, one can build the most general renormalizable $SU(2)_L \times U(1)_Y$ gauge invariant Higgs potential [20–27]:

$$\begin{aligned} V_{\text{Higgs}}(\Phi_1, \Phi_2) = & \frac{\lambda_1}{2}(\Phi_1^\dagger \Phi_1)^2 + \frac{\lambda_2}{2}(\Phi_2^\dagger \Phi_2)^2 + \lambda_3(\Phi_1^\dagger \Phi_1)(\Phi_2^\dagger \Phi_2) + \lambda_4(\Phi_1^\dagger \Phi_2)(\Phi_2^\dagger \Phi_1) \\ & + \frac{1}{2} \left[\lambda_5(\Phi_1^\dagger \Phi_2)^2 + \text{h.c.} \right] + \left\{ \left[\lambda_6(\Phi_1^\dagger \Phi_1) + \lambda_7(\Phi_2^\dagger \Phi_2) \right] (\Phi_1^\dagger \Phi_2) + \text{h.c.} \right\} \\ & - \frac{1}{2} \left\{ m_{11}^2 \Phi_1^\dagger \Phi_1 + \left[m_{12}^2 \Phi_1^\dagger \Phi_2 + \text{h.c.} \right] + m_{22}^2 \Phi_2^\dagger \Phi_2 \right\}. \end{aligned} \quad (2.1)$$

By hermiticity of eq. (2.1), $\lambda_{1,2,3,4}$, as well as m_{11} and m_{22} are real-valued; while the dimensionless parameters λ_5 , λ_6 , λ_7 and m_{12}^2 are in general complex.

2.1.1 Mass eigenstates

After the $SU(2)_L \times U(1)_Y$ gauge symmetry is broken down to $U(1)_{\text{em}}$ via the Higgs mechanism, one can choose a basis where the vacuum expectation values (VEVs) of the two Higgs doublets, v_1 and v_2 are non-zero, real and positive, and fix the following parameterization [28, 29]:

$$\Phi_1 = \begin{pmatrix} \varphi_1^+ \\ (v_1 + \eta_1 + i\chi_1)/\sqrt{2} \end{pmatrix}, \quad \Phi_2 = \begin{pmatrix} \varphi_2^+ \\ (v_2 + \eta_2 + i\chi_2)/\sqrt{2} \end{pmatrix}. \quad (2.2)$$

Here $\eta_{1,2}$ and $\chi_{1,2}$ are neutral scalar fields and $\varphi_{1,2}^\pm$ are charged scalar fields. The physical Higgs eigenstates are obtained as follows.

The charged Higgs fields H^\pm and the charged would-be Goldstone boson fields G^\pm are a mixture of the charged components of the Higgs doublets (2.2), $\varphi_{1,2}^\pm$:

$$\begin{aligned} H^\pm &= -\sin \beta \varphi_1^\pm + \cos \beta \varphi_2^\pm, \\ G^\pm &= \cos \beta \varphi_1^\pm + \sin \beta \varphi_2^\pm, \end{aligned} \quad (2.3)$$

where the mixing angle β is defined through the ratio of the VEVs of the two Higgs doublets Φ_2 and Φ_1 , $\tan \beta = v_2/v_1$. G^\pm give masses to the W^\pm bosons.

Obtaining the neutral physical Higgs states is a few steps procedure. First, one rotates the imaginary parts of the neutral components of eq. (2.2): (χ_1, χ_2) into the basis (G^0, η_3) :¹

$$\begin{aligned} G^0 &= \cos \beta \chi_1 + \sin \beta \chi_2, \\ \eta_3 &= -\sin \beta \chi_1 + \cos \beta \chi_2, \end{aligned} \quad (2.4)$$

¹Note that in the case of $m_{12}^2 = \lambda_6 = \lambda_7 = 0$ and all other parameters of eq. (2.1) are real, the physical Higgs sector of the 2HDM is analogous to the one of the tree-level MSSM. In this case the scalar field η_3 is equivalent to the MSSM neutral CP-odd Higgs boson A^0 .

where G^0 is the would-be Goldstone boson which gives a mass to the Z gauge boson. After elimination of the Goldstone mode, the remaining neutral CP-odd component η_3 mixes with the neutral CP-even components $\eta_{1,2}$. The relevant squared mass matrix $\mathcal{M}_{ij}^2 = \partial^2 V_{\text{Higgs}} / (\partial \eta_i \partial \eta_j)$, $i, j = 1, 2, 3$, has to be rotated from the so called "weak basis" (η_1, η_2, η_3) to the diagonal basis (H_1^0, H_2^0, H_3^0) by an orthogonal 3×3 matrix \mathcal{R} as follows:

$$\mathcal{R} \mathcal{M}^2 \mathcal{R}^T = \mathcal{M}_{\text{diag}}^2 = \text{diag}(M_{H_1^0}^2, M_{H_2^0}^2, M_{H_3^0}^2), \quad (2.5)$$

with

$$\begin{pmatrix} H_1^0 \\ H_2^0 \\ H_3^0 \end{pmatrix} = \mathcal{R} \begin{pmatrix} \eta_1 \\ \eta_2 \\ \eta_3 \end{pmatrix}, \quad (2.6)$$

where we have defined the Higgs fields H_i^0 such that their masses satisfy the inequalities:

$$M_{H_1^0} \leq M_{H_2^0} \leq M_{H_3^0}. \quad (2.7)$$

Note that the mass eigenstates H_i^0 have a mixed CP structure.

Following [30], we parametrize the orthogonal 3×3 matrix \mathcal{R} by three rotation angles α_i , $i = 1, 2, 3$:

$$\begin{aligned} \mathcal{R} &= \begin{pmatrix} 1 & 0 & 0 \\ 0 & \cos \alpha_3 & \sin \alpha_3 \\ 0 & -\sin \alpha_3 & \cos \alpha_3 \end{pmatrix} \begin{pmatrix} \cos \alpha_2 & 0 & \sin \alpha_2 \\ 0 & 1 & 0 \\ -\sin \alpha_2 & 0 & \cos \alpha_2 \end{pmatrix} \begin{pmatrix} \cos \alpha_1 & \sin \alpha_1 & 0 \\ -\sin \alpha_1 & \cos \alpha_1 & 0 \\ 0 & 0 & 1 \end{pmatrix} \\ &= \begin{pmatrix} c_1 c_2 & s_1 c_2 & s_2 \\ -(c_1 s_2 s_3 + s_1 c_3) & c_1 c_3 - s_1 s_2 s_3 & c_2 s_3 \\ -c_1 s_2 c_3 + s_1 s_3 & -(c_1 s_3 + s_1 s_2 c_3) & c_2 c_3 \end{pmatrix}, \end{aligned} \quad (2.8)$$

with $s_i = \sin \alpha_i$ and $c_i = \cos \alpha_i$, which we vary in our numerical analysis in the following ranges:

$$-\frac{\pi}{2} < \alpha_1 \leq \frac{\pi}{2}; \quad -\frac{\pi}{2} < \alpha_2 \leq \frac{\pi}{2}; \quad 0 \leq \alpha_3 \leq \frac{\pi}{2}. \quad (2.9)$$

2.2 Z_2 symmetry and input parameter set

In the most general 2HDM, some types of Yukawa interactions can introduce flavour changing neutral currents (FCNC) already at tree level. It is well known that the latter effects are small in nature. This problem has been solved by imposing a discrete Z_2 symmetry on the Lagrangian. It forbids $\Phi_1 \leftrightarrow \Phi_2$ transitions and in its exact form it also leads to conservation of CP [31]. In order to allow some effects of CPV it is necessary to violate the Z_2 symmetry. Basically, there are two ways of Z_2 symmetry violation – "soft" and "hard". A softly broken Z_2 symmetry suppresses FCNC at tree level, but still allows CPV.

In this paper we will work in a model of a softly broken Z_2 symmetry of the 2HDM Lagrangian. This forbids the quartic terms proportional to λ_6 and λ_7 in eq. (2.1), but the quadratic term with m_{12}^2 is still allowed [32, 33]:

$$\begin{aligned} V_{\text{Higgs}}^{\text{soft}}(\Phi_1, \Phi_2) &= \frac{\lambda_1}{2} (\Phi_1^\dagger \Phi_1)^2 + \frac{\lambda_2}{2} (\Phi_2^\dagger \Phi_2)^2 + \lambda_3 (\Phi_1^\dagger \Phi_1) (\Phi_2^\dagger \Phi_2) + \lambda_4 (\Phi_1^\dagger \Phi_2) (\Phi_2^\dagger \Phi_1) \\ &+ \frac{1}{2} \left[\lambda_5 (\Phi_1^\dagger \Phi_2)^2 + \text{h.c.} \right] - \frac{1}{2} \left\{ m_{11}^2 \Phi_1^\dagger \Phi_1 + \left[m_{12}^2 \Phi_1^\dagger \Phi_2 + \text{h.c.} \right] + m_{22}^2 \Phi_2^\dagger \Phi_2 \right\}. \end{aligned} \quad (2.10)$$

The Higgs potential (2.10) has 12 real parameters: 2 real masses: $m_{11,22}^2$, 2 VEVs: $v_{1,2}$, four real quartic couplings: $\lambda_{1,2,3,4}$ and two complex parameters: λ_5 and m_{12}^2 . The conditions for having an extremum of eq. (2.10) reduce the number of parameters: $m_{11,22}^2$ are eliminated by the minimization conditions, and the combination $v_1^2 + v_2^2$ is fixed at the electroweak scale $v = (\sqrt{2}G_F)^{-1/2} = 246$ GeV. Moreover, in this case the minimization conditions also relates $\text{Im}(m_{12}^2)$ and $\text{Im}(\lambda_5)$:

$$\text{Im}(m_{12}^2) = v_1 v_2 \text{Im}(\lambda_5). \quad (2.11)$$

Thus, our Higgs potential (2.10) is a function of 8 real independent parameters:

$$\{\lambda_{1,2,3,4}, \text{Re}(\lambda_5), \text{Re}(m_{12}^2), \tan\beta, \text{Im}(m_{12}^2)\}. \quad (2.12)$$

It contains minimal CPV generated by $m_{12}^2 \neq 0$ and complex. In our further analysis we will use the following parameter set equivalent to eq. (2.12):

$$\left\{M_{H_1^0}, M_{H_2^0}, M_{H^+}, \alpha_1, \alpha_2, \alpha_3, \tan\beta, \text{Re}(m_{12})\right\}. \quad (2.13)$$

Note that the mass of the heaviest neutral Higgs boson H_3^0 is not an independent parameter. In the considered CP violating case, the matrix elements $(\mathcal{M}^2)_{13}$ and $(\mathcal{M}^2)_{23}$ of the squared mass matrix (2.5) are non-zero and correlated [34]:

$$(\mathcal{M}^2)_{13} = \tan\beta (\mathcal{M}^2)_{23}. \quad (2.14)$$

Writing this relation in terms of the physical masses $M_{H_1^0}, M_{H_2^0}, M_{H_3^0}$ one obtains [34]:

$$M_{H_3^0}^2 = \frac{M_{H_1^0}^2 R_{13}(R_{12} \tan\beta - R_{11}) + M_{H_2^0}^2 R_{23}(R_{22} \tan\beta - R_{21})}{R_{33}(R_{31} - R_{32} \tan\beta)}, \quad (2.15)$$

where $R_{ij}, i, j = 1, 2, 3$, are the elements of the rotation matrix (2.8).

The expressions for the parameters $\lambda_{1,2,3,4}, \text{Re}\lambda_5, \text{Im}\lambda_5$ of the scalar potential (2.10) as functions of the physical masses and mixing angles are given in appendix B.

In appendix C we also list the triple scalar couplings of the Higgs bosons calculated from the potential (2.10) and relevant to our study. Note, that the couplings $\mathcal{C}(H_i^0 H^\pm G^\mp)$, $i = 1, 2, 3$, have both real and imaginary parts and can lead to CPV.

2.3 Higgs and gauge boson interactions

The Higgs and gauge boson interactions arise from the covariant derivatives of the doublet fields $\Phi_{1,2}$:

$$\mathcal{L}_{\text{gauge}} = \sum_{i=1}^2 (D^\mu \Phi_i)^\dagger (D_\mu \Phi_i), \quad D^\mu = \partial^\mu + ig \vec{T}_a \vec{W}_\mu^a + ig' Y_i B_\mu / 2 \quad (2.16)$$

where \vec{T}_a are the isospin generators, Y_i are the hypercharges of the Higgs Φ_i , \vec{W}_μ^a and B_μ are the $\text{SU}(2)_L$ and $\text{U}(1)_Y$ gauge fields, g, g' are the corresponding $\text{SU}(2)_L$ and $\text{U}(1)_Y$ gauge couplings.

After having rotated the Higgs and gauge bosons fields to their mass eigenstates bases one obtains terms of triple and quartic interactions between them. The interactions relevant to our study are $H_i^0 WW$ and $H_i^0 W^\pm H^\mp$, with the corresponding couplings

$$\begin{aligned}\mathcal{C}(H_i^0 WW) &= \cos \beta R_{i1} + \sin \beta R_{i2}, \\ \mathcal{C}(H_i^0 W^\pm H^\mp) &= \mp i(\sin \beta R_{i1} - \cos \beta R_{i2}) \pm R_{i3}.\end{aligned}\quad (2.17)$$

Note that $\mathcal{C}(H_i^0 WW)$ is purely real, while $\mathcal{C}(H_i^0 W^\pm H^\mp)$ has both real and imaginary parts and can lead to effects of CPV, as we will see later. The relevant Lagrangian is given in appendix C.

From the condition for unitarity of the rotation matrix \mathcal{R} one derives the following sum rules:

$$\mathcal{C}(H_i^0 WW)^2 + |\mathcal{C}(H_i^0 W^+ H^-)|^2 = 1 \quad \text{for each } i = 1, 2, 3 \quad (2.18)$$

$$\sum_{i=1}^3 \mathcal{C}(H_i^0 WW)^2 = 1 \quad (2.19)$$

From eqs. (2.18) and (2.17) follows that if for a fixed i the term $|\mathcal{C}(H_i^0 W^+ H^-)|^2$ is suppressed, then $(\sin \beta R_{i1} - \cos \beta R_{i2})^2 \approx 0$ and $R_{i3}^2 \approx 0$. The relation $R_{i3}^2 \approx 0$ implies that H_i^0 has a very small pseudoscalar component and is dominantly a CP-even state. Furthermore, the sum rule (2.19) implies that the other Higgs states decouple, i.e. $\mathcal{C}(H_j^0 WW)^2 \approx 0$ for $j \neq i$. We will come back to the physical consequences of these sum rules in our physics discussion on the studied decay and production processes in section 4.

2.4 Yukawa interactions

In the framework of the 2HDM various models of Yukawa interactions can be realized [4]. Depending on the Yukawa interaction one distinguishes between different types of 2HDM's.

The most general 2HDM, in which each fermion doublet and singlet couples to both Higgs doublets is called the type-III model. This model leads to FCNC already at tree level and is a subject of severe constraints from flavour physics observables [21, 35]. As we already discussed, in order to avoid problems with FCNC usually a Z_2 discrete symmetry is imposed on the Lagrangian [31].

In the 2HDM type-I all fermions, quarks and leptons, couple to only one of the Higgs doublets exactly like in the SM. These models are interesting as the decoupling Higgs is a natural candidate for dark matter.

There exists another type of 2HDM where one of the Higgs doublets couples to leptons and the other one to the up and down quarks [36–38]. The phenomenology of these models has been reviewed recently in [39–41].

In the present paper we work in type-II 2HDM. In this model, down-type quarks and charged leptons couple to Φ_1 and the up-type quarks couple to the other Higgs doublet Φ_2 . (In the MSSM the Higgs sector is also a 2HDM type-II, but with the Higgs self-interactions fixed by gauge couplings.) In order to avoid FCNC at tree level, but allow for CPV, our discrete Z_2 symmetry is softly broken, i.e. $\lambda_6 = \lambda_7 = 0$, but m_{12}^2 is non-zero and complex, see section 2.2.

The parts of the interaction Lagrangian of Higgs bosons and fermions relevant for our discussions are given in appendix C. Since the neutral Higgses are mixtures of CP-odd and CP-even states, their couplings to a fermion pair have the general form $a + i b \gamma_5$ with a and b real, that can lead to CPV.

2.5 Theoretical constraints on the Higgs potential

The Higgs potential $V_{\text{Higgs}}^{\text{soft}}$ given by eq. (2.10) has to satisfy some general requirements like positivity, unitarity and perturbativity [30]. These requirements together with the minimum conditions naturally lead to constraints on its parameters [28, 30, 34]. The theoretical constraints on the potential (2.10) are well studied and will not be a subject of this note. For completeness, we list below the expressions we have implemented in our numerical code.

In order to have a stable vacuum the potential should be positive for large values of $|\phi_k|$, which leads to the constraints [28]:

$$\lambda_1 > 0, \quad \lambda_2 > 0, \quad \lambda_3 + \sqrt{\lambda_1 \lambda_2} > 0, \quad \lambda_4 + \lambda_4 - |\lambda_5| + \sqrt{\lambda_1 \lambda_2} > 0. \quad (2.20)$$

From the requirement that theory remains perturbative we have: $|\lambda_i| \leq 8\pi$ for any i . The unitarity requirement means that the tree-level amplitudes for Higgs-Higgs, Higgs-vector boson and vector boson-vector boson scattering should not exceed the unitarity limit when contributing to the s-wave. Both unitarity and perturbativity requirements lead to the constraints [28]:

$$\begin{aligned} \left| \frac{1}{2} \left(\lambda_1 + \lambda_2 \pm \sqrt{(\lambda_1 - \lambda_2)^2 + 4|\lambda_5|^2} \right) \right| &< 8\pi, \\ \left| \frac{1}{2} \left(\lambda_1 + \lambda_2 \pm \sqrt{(\lambda_1 - \lambda_2)^2 + 4\lambda_4^2} \right) \right| &< 8\pi, \\ \left| \frac{3(\lambda_1 + \lambda_2) \pm \sqrt{9(\lambda_1 - \lambda_2^2 + 4(\lambda_3 + \lambda_4)^2)}}{2} \right| &< 8\pi, \\ |\lambda_3 \pm \lambda_4| < 8\pi, \quad |\lambda_3 \pm |\lambda_5|| < 8\pi, \quad |\lambda_3 + 2\lambda_4 \pm |\lambda_5|| < 8\pi. \end{aligned} \quad (2.21)$$

As the eqs. (2.20) and (2.21) only depend on the absolute value of λ_5 , they do not constrain the phase of λ_5 . We will see later, that these theoretical constraints already strongly reduce the C2HDM parameter space [28, 30, 34].

3 CP violation in H^\pm production and decays

3.1 The processes

We study CPV induced by one-loop corrections in the C2HDM in the following processes involving the charged Higgs boson:

- Decays:

$$H^\pm \rightarrow tb, \quad H^\pm \rightarrow W^\pm H_i, \quad i = 1, 2. \quad (3.1)$$

- Associated production with a top quark at the LHC:

$$pp \rightarrow H^\pm t + X, \quad (3.2)$$

with the partonic subprocesses:

$$b g \rightarrow t H^- \quad \text{and} \quad \bar{b} g \rightarrow \bar{t} H^+. \quad (3.3)$$

- Charged Higgs production (3.2) plus subsequent decays (3.1).

The tree-level graphs of the considered processes for H^- are shown in figure 1.

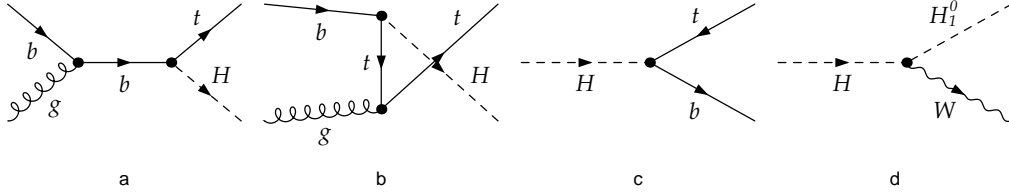


Figure 1. The tree-level graphs for $bg \rightarrow tH^-$: a) s-channel, b) t-channel, and charged Higgs decays: c) $H^- \rightarrow \bar{t}b$, d) $H^- \rightarrow W^- H_1^0$.

3.2 CP violating asymmetries

For the processes listed in section (3.1) we investigate the following CP violating H^\pm rate asymmetries:

- Decay rate asymmetries $A_{D,f}^{CP}$, defined by:

$$A_{D,f}^{CP} (H^\pm \rightarrow f) = \frac{\Gamma(H^+ \rightarrow f) - \Gamma(H^- \rightarrow \bar{f})}{2\Gamma^{\text{tree}}(H^+ \rightarrow f)}, \quad (3.4)$$

where D stands for decay and f stands for any of the decay modes: $f = t\bar{b}$; $W^\pm H_i^0$ with $i = 1, 2$.

- Production rate asymmetry A_P^{CP} , related only to the process (3.2) and defined by:

$$A_P^{CP} = \frac{\sigma(pp \rightarrow H^+ \bar{t}) - \sigma(pp \rightarrow H^- t)}{2\sigma^{\text{tree}}(pp \rightarrow H^+ \bar{t})}, \quad (3.5)$$

where P stands for production.

- Asymmetries A_f^{CP} for the combined processes of production and subsequent decays, defined by:

$$A_f^{CP} = \frac{\sigma(pp \rightarrow \bar{t}H^+ \rightarrow \bar{t}f) - \sigma(pp \rightarrow tH^- \rightarrow tf)}{2\sigma^{\text{tree}}(pp \rightarrow \bar{t}H^+ \rightarrow \bar{t}f)}. \quad (3.6)$$

In [13] we have shown that in narrow width approximation, when the decay width of H^+ is much smaller than its mass, the total asymmetry A_f^{CP} given by eq. (3.6) is an algebraic

sum of the asymmetry A_P^{CP} in the production and the asymmetry $A_{D,f}^{CP}$ in the decay f of the charged Higgs boson:

$$A_f^{CP} = A_P^{CP} + A_{D,f}^{CP}. \quad (3.7)$$

The decay asymmetries (3.4) might be of interest for the ILC, where CPV can occur only in the H^\pm decays. Since the measurements on $b \rightarrow s\gamma$ put a stringent lower limit on the charged Higgs mass $M_{H^\pm} > 295$ GeV, the decay modes (3.1) are dominant.

3.3 CP violating loop contributions

In order to get CPV using the asymmetries introduced in section 3.2, we need both non-zero CP violating phases in the Lagrangian and CP conserving phases (strong phases) in the absorptive parts of the one-loop amplitudes.

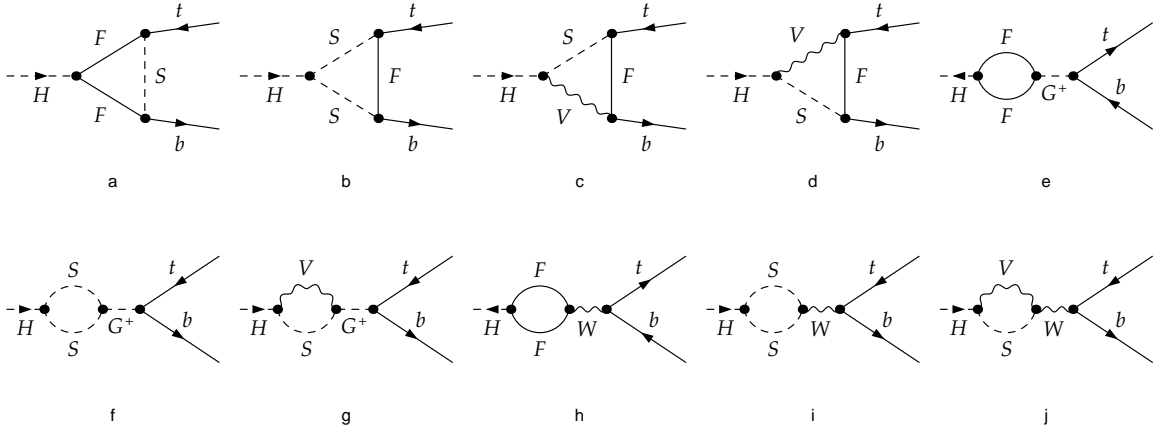


Figure 2. Generic CP violating selfenergy and vertex contributions to $H^- \rightarrow t\bar{b}$. F denotes a generic fermion, S a generic neutral or charged scalar field, and V a generic vector boson.

In the C2HDM, the CP violating phases arise from:

- Neutral Higgs couplings to a fermion pair
- Charged Higgs – Neutral Higgs – gauge bosons couplings
- Charged Higgs – Neutral Higgs – Goldstone bosons couplings

The parts of the C2HDM Lagrangian needed for this study are given in the appendix C.

The CP conserving phases originate from various on-shell intermediate states of the one-loop amplitudes. For the considered H^\pm production and decay processes, the strong phases coming from cuts e.g. in $t \rightarrow bW^\pm$ and $H_1^0 \rightarrow b\bar{b}$ will always contribute, while the strong phases coming from cuts in $H^\pm \rightarrow W^\mp H_i^0$, $H^\pm \rightarrow G^\mp H_i^0$, $H^\pm \rightarrow t\bar{b}$, etc. in the loops, will contribute only if they are kinematically allowed. All possible generic CP

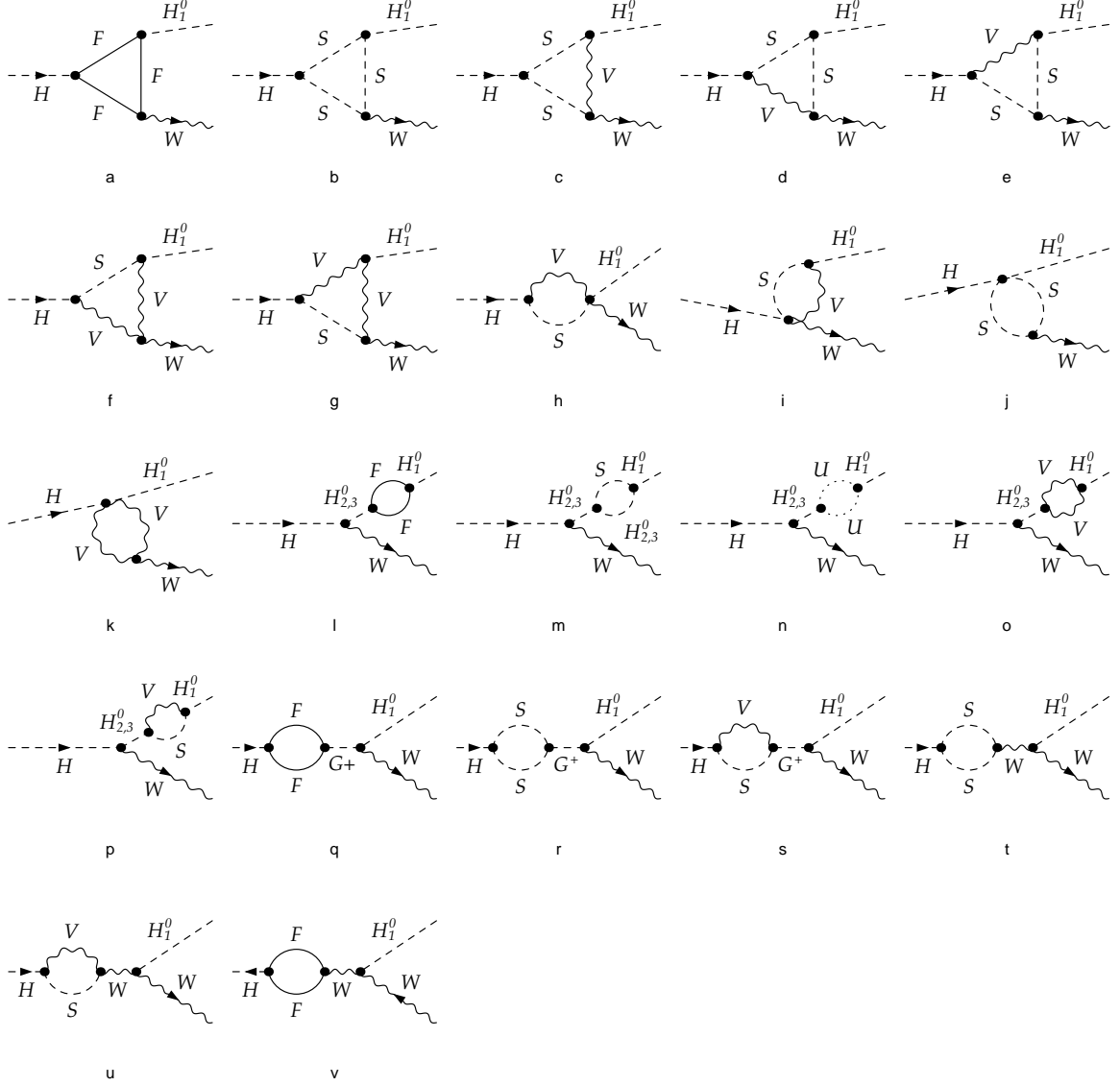


Figure 3. Generic CP violating selfenergy and vertex contributions to $H^- \rightarrow W^- H_1^0$.

violating one-loop contributions to the decay $H^\pm \rightarrow t\bar{b}$ are shown in figure 2 and to the decay $H^\pm \rightarrow W^\pm H_1^0$ in figure 3.

Furthermore, we have three types of possible generic CP violating loop contributions to the partonic cross sections of the production processes (1.1): selfenergy contributions, shown in figure 4; vertex contributions shown in figure 5 and box diagram contributions shown in figure 6. All diagrams have been generated with FA [16] package, for which we

have written a complete model file for the C2HDM, see Appendices D.1 and D.2 for details.

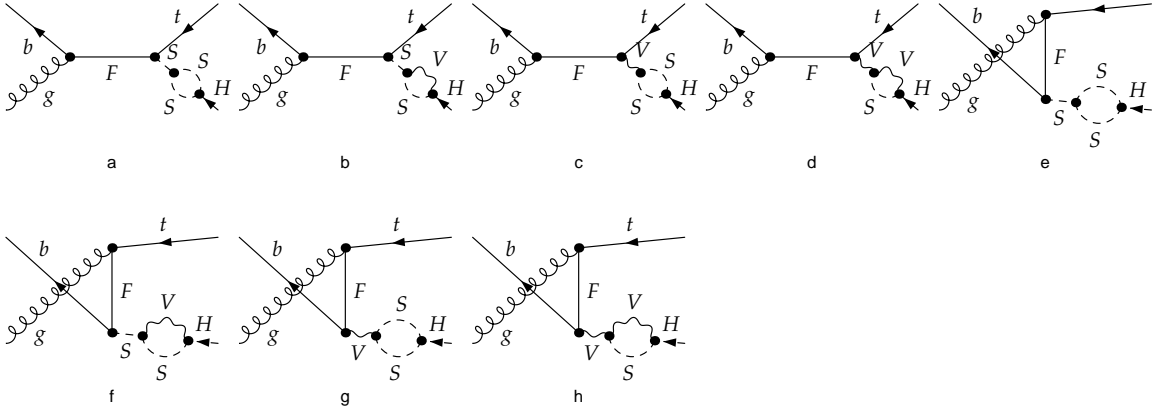


Figure 4. Generic CP violating selfenergy contributions to charged Higgs boson production $\bar{b} g \rightarrow H^+ \bar{t}$.

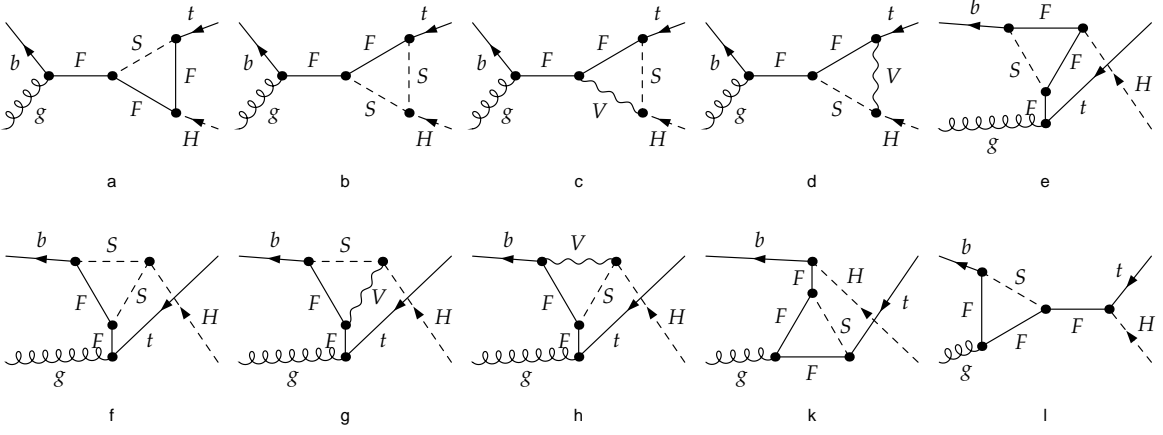


Figure 5. Generic CP violating vertex contributions to charged Higgs boson production $\bar{b} g \rightarrow H^+ \bar{t}$.

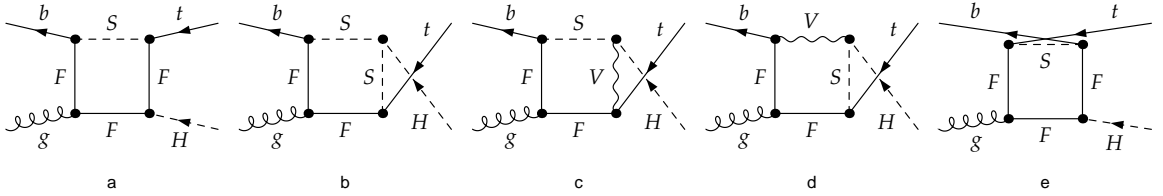


Figure 6. Generic CP violating box contributions to charged Higgs boson production $\bar{b} g \rightarrow H^+ \bar{t}$.

4 Numerical results

In this section we present our numerical results for the CP violating asymmetries (3.4), (3.5) and (3.6) in the C2HDM with a softly broken Z_2 symmetry (2.10). All calculations have been done using the packages FA and FC [16], for which we have written a complete FA model file and have extended the corresponding FC fortran drivers for the C2HDM. The implementation is described for the FA model file in the appendix D.1 and for the FC fortran drivers in D.2. In our numerical analysis we also have used LoopTools [42–44]. The calculations are done in the 'tHooft-Feynman gauge using dimensional regularization. However, we stress that we do not renormalize any parameters or fields since our CPV rate asymmetries involve only the imaginary parts of the loop integrals which are always finite. For the evaluation of the PDF's we use CTEQ5L, with α_s , calculated at the scale $Q = \sqrt{\hat{s}}$.

In this paper we work with the following set of real input parameters [30], see section 2.2:

$$\left\{ M_{H_1^0}, M_{H_2^0}, M_{H^\pm}, \alpha_1, \alpha_2, \alpha_3, \tan \beta, \text{Re}(m_{12}) \right\}. \quad (4.1)$$

In the literature often the parameter μ is used instead of $\text{Re}(m_{12})$:

$$\mu^2 = \frac{v^2}{2v_1 v_2} \text{Re}(m_{12}^2), \quad v^2 = v_1^2 + v_2^2. \quad (4.2)$$

The expressions for the parameters of the scalar potential (2.10), λ_i , $i = 1, 2, 3, 4, 5$, as functions of the physical masses, mixing angles and μ [34] are given in appendix B. For the values of the SM parameters used we refer to [45], except for the top mass, taken from the last Tevatron measurement [46]:

$$m_t = 173.1 \text{ GeV}, \quad m_b = 4.7 \text{ GeV}, \quad \text{and} \quad \alpha = 1/137.03599. \quad (4.3)$$

Furthermore, we would like to add some comments on the existing constraints on the values of the C2HDM parameters. Basically they come from:

- theory – these are the requirements for positivity and unitarity of the Higgs potential, see section 2.5
- experiment – mainly coming from the electroweak precision data at LEP. These constraints we will discuss in the next subsection

4.1 Experimental constraints

In principle, there is quite a long list of experimental bounds to constrain the phenomenology of the 2HDM. Examples are: B-mixing/B-decays constraints, LEP2 non-discovery constraints, direct searches for H^\pm , muon anomalous magnetic moment, electron electric dipole moment (EDM), etc., see [30, 33, 47, 48] and the references therein. Many of these constraints are strongly dependent on the model of Yukawa interactions, on the considered process and on the related parameter space. As already mentioned, the theoretical constraints described in section 2.5 already strongly reduce the parameter space of the C2HDM [48]. In [35] the authors combine these constraints with the existing experimental

constraints and review the "profile of the surviving parameter space" of the type II 2HDM. There they show that large values of $\tan\beta$ are forbidden by the unitarity constraints, see section 2.5, except for the case $M_{H_1^0} < \mu$ [35]. Furthermore, they show that the experimental constraints also usually exclude parameter regions for $\tan\beta \sim 10$ [35]. However, in principle it can be shown that one can fine-tune the parameters to allow some tiny parameter regions for large $\tan\beta$ [49].

Among the experimental constraints we consider the following ones, which have the strongest impact on restricting the general 2HDM parameter space:

- For the lightest neutral Higgs boson we take into account the LEP2 non-discovery bound, $M_{H_1^0} > 114.4$ GeV [50].
- In addition to the lower bounds from the CERN LEP and Tevatron direct searches [51–54], the charged Higgs mass is quite severely constrained by the $B \rightarrow X_s \gamma$ data [55–61]. At the next-to-next-to-leading order in the type-II 2HDM it implies that $M_{H^\pm} \geq 295$ GeV, [59–61]. In our analysis we follow the latter lower bound.
- Another important experimental constraint, coming from the electroweak physics, is related to the precise determination of the ρ -parameter [62]. Its deviation $\Delta\rho$ from the SM value should accommodate all new physics contributions. $\Delta\rho$ is constrained by the error of the measured value of the parameter ρ_0 , which at the 2σ level is [50]:

$$\rho_0 = 1.0004 \begin{smallmatrix} +0.0029 \\ -0.0011 \end{smallmatrix} . \quad (4.4)$$

In our numerical code we implement the expressions for $\Delta\rho$ given in [30], with the requirement:

$$-0.0011 \leq \Delta\rho \leq 0.0029 . \quad (4.5)$$

The analytic expressions for the extra contributions in $\Delta\rho$ in the framework of the C2HDM are given in appendix A.

4.2 CP violation in H^\pm -decays

We discuss the CPV decay rate asymmetries $A_{D,f}^{CP}$, given with eq. (3.4), for the decays $H^\pm \rightarrow t\bar{b}$ and $H^\pm \rightarrow W^\pm H_i^0$, $i = 1, 2$. Note that we do not consider the decay mode $H^\pm \rightarrow W^\pm H_3^0$ as a possible measurable channel for the CPV asymmetry due to its tiny branching ratio (BR) in the considered parameter ranges.

In figure 7, figure 8 and figure 9 we present the CP asymmetries $A_{D,tb}^{CP}$, $A_{D,WH_1^0}^{CP}$ and $A_{D,WH_2^0}^{CP}$, respectively, as functions of the charged Higgs mass, for several values of $\tan\beta$. The curves in the figures are cut once any of the parameter constraints discussed in section 2.5 and section 4.1 is violated. In particular, in the considered parameter range, the $\Delta\rho$ constraint imposes that the charged Higgs mass M_{H^\pm} cannot acquire large values: in figure 7, for $\tan\beta = 1.5$, M_{H^\pm} cannot exceed the limit of ≈ 368 GeV, while for $\tan\beta = 4.5$: $M_{H^\pm} \lesssim 408$ GeV, etc..

All discussed CPV asymmetries exhibit a mild dependence on M_{H^\pm} and a strong dependence on $\tan\beta$: $A_{D,tb}^{CP}$ increases, while $A_{D,WH_1^0}^{CP}$ and $A_{D,WH_2^0}^{CP}$ strongly decrease when $\tan\beta$ increases. This is shown in figures 7, 8, and 9.

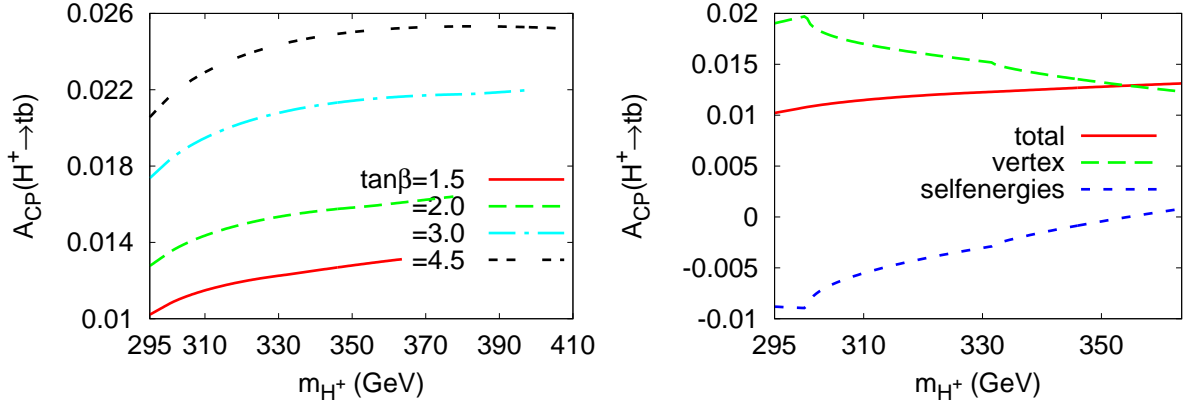


Figure 7. Left: CPV asymmetry $A_{D,tb}^{CP}$ as a function of M_{H^+} for four values of $\tan\beta$. The other parameters are: $M_{H_1^0} = 120$ GeV, $M_{H_2^0} = 220$ GeV, $\text{Re}(m_{12}) = 170$ GeV, $\alpha_1 = 0.8$, $\alpha_2 = -0.9$ and $\alpha_3 = \pi/3$. Right: CPV vertex and selfenergy contributions to $A_{D,tb}^{CP}$, as functions of the charged Higgs mass for $\tan\beta = 1.5$.

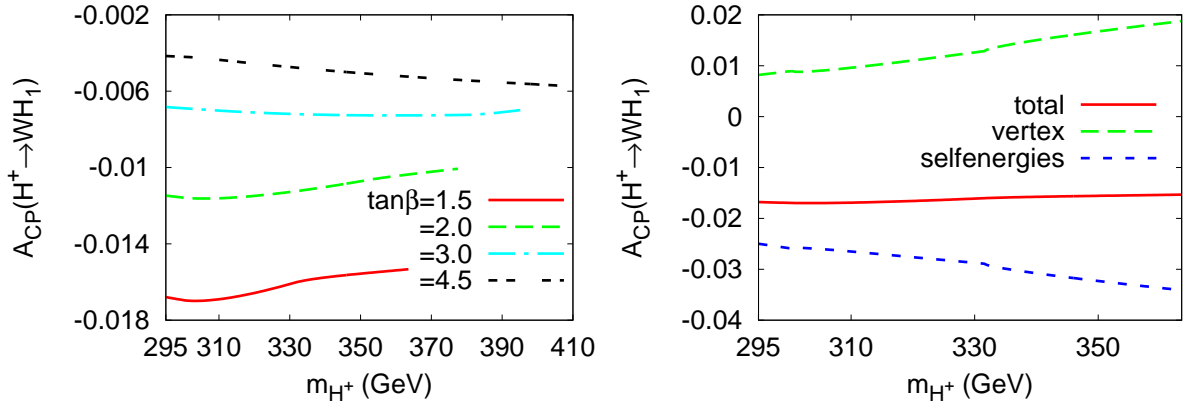


Figure 8. Left: CPV asymmetry $A_{D,WH_1^0}^{CP}$ as a function of M_{H^+} for four values of $\tan\beta$. The other parameters are the same as for figure 7. Right: CPV vertex and selfenergy contributions to $A_{D,WH_1^0}^{CP}$, as functions of the charged Higgs mass for $\tan\beta = 1.5$.

As we already commented in section 4.1 large values of $\tan\beta$ are excluded, except for some small areas in the region $M_{H_1^0} < \mu$ which require fine-tuning of the parameters [35]. Moreover, we have checked that very often for large $\tan\beta$ the mass of the heaviest Higgs boson $M_{H_3^0}$ becomes tachyonic. Therefore in most of the cases we show numerical results for $\tan\beta$ in the range $1.5 \div 4.5$.

In figure 7 we see that the asymmetry $A_{D,tb}^{CP}$ is positive and can reach $\sim 2.5\%$ for $\tan\beta = 4.5$ and $M_{H^+} \approx 400$ GeV. In the same figure we show the vertex and the selfenergy contributions in $A_{D,tb}^{CP}$ for $\tan\beta = 1.5$. The figure shows that these contributions enter with opposite signs and there is a partial cancellation between them. In contrast to the MSSM,

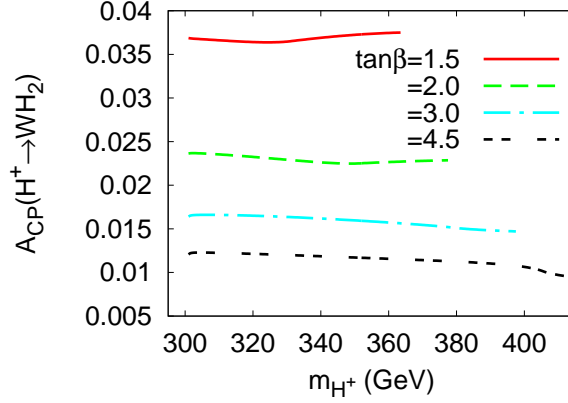


Figure 9. CPV asymmetry A_{D,WH_2}^{CP} (3.4), as a function of M_{H^+} for four values of $\tan\beta$. The other parameters are: $M_{H_1^0} = 120$ GeV, $M_{H_2^0} = 220$ GeV, $\text{Re}(m_{12}) = 170$ GeV, $\alpha_1 = 0.8$, $\alpha_2 = -0.9$ and $\alpha_3 = \pi/3$.

here the dominant contribution in the CPV asymmetry comes from the vertex diagrams.

For the bosonic channel $H^\pm \rightarrow W^\pm H_1^0$, the CPV asymmetry is shown in figure 8. It is seen that $A_{D,WH_1^0}^{CP}$ is negative and can reach $\sim 1.7\%$ for $\tan\beta = 1.5$ and M_{H^+} close to the lower limit ≈ 297 GeV. In this channel there is also a cancellation between the selfenergy and the vertex contributions, which is shown in the figure. In the CPV decay asymmetry $A_{D,WH_1^0}^{CP}$ the dominant contribution stems from the selfenergies.

In figure 9 we show the asymmetry $A_{D,WH_2^0}^{CP}$ as a function of the charged Higgs mass. In contrast to the other bosonic channel $H^\pm \rightarrow WH_1^0$, it is positive and the absolute value is larger. For $\tan\beta = 1.5$, it is almost constant $\sim 3.7\%$. For this asymmetry we do not show explicitly the individual contributions. However, we would like to note, that cancellation occurs between the vertex and the selfenergy contributions. Similar to the decay into H_1^0 the selfenergy contributions are dominant in $A_{D,WH_2^0}^{CP}$.

In all three discussed cases we have checked that the influence of the CKM matrix is very small, therefore we work with a diagonal one.

In figure 10 we show a scan over the parameters α_1 and α_2 , in order to illustrate the allowed domain for (α_1, α_2) together with the size of the CPV asymmetry in the $H^\pm \rightarrow t\bar{b}$ decay. As we already mentioned, the excluded parameter regions are due to the combination of all theoretical and experimental constraints: vacuum stability, unitarity, large additional contributions to $\Delta\rho$, as well as tachyonic modes of $M_{H_3^0}$ or violation of the ordering $M_{H_1^0} \leq M_{H_2^0} \leq M_{H_3^0}$. In the figure we see that for smaller values of $\tan\beta$ the allowed domain is larger and almost vanishes for $\tan\beta = 4.5$ and that the CPV asymmetry $A_{D,tb}^{CP}$ exceeds 2% only in some small areas.

In figure 11 we show a similar scan for the $H^\pm \rightarrow W^\pm H_1^0$ decay. When we scan over α_1 and α_2 for a fixed value of α_3 , we find a region where the coupling $\mathcal{C}(H_1^0 H^\pm W^\mp)$ becomes very small. It is seen in the figure that for $\tan\beta = 1.5$ $\mathcal{C}(H_1^0 H^\pm W^\mp) \rightarrow 0$ for

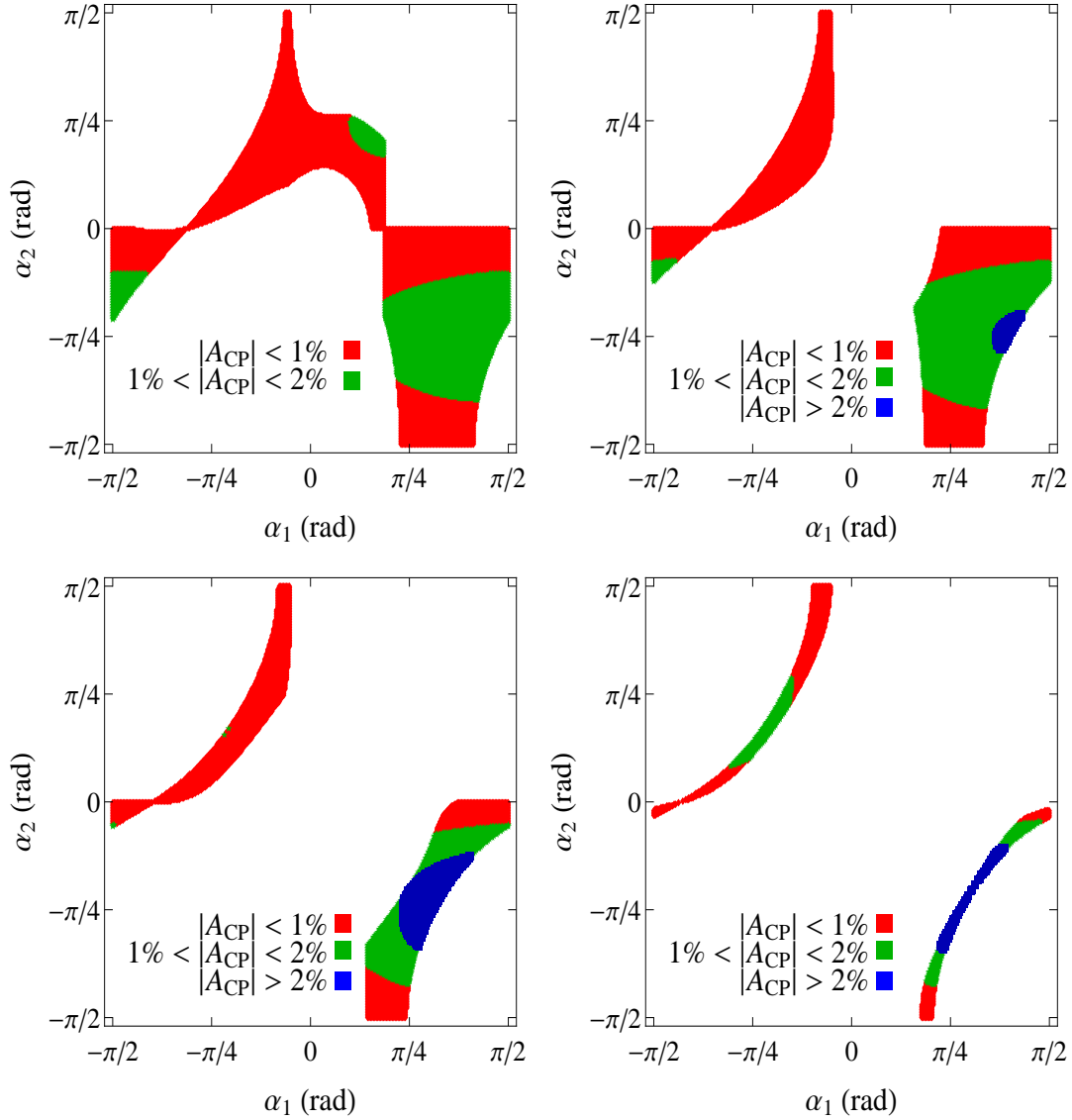


Figure 10. The allowed parameter regions in the (α_1, α_2) plan in the C2HDM together with the absolute value of the CPV asymmetry $A_{D, tb}^{CP}$. We have taken $M_{H_1^0} = 120$ GeV, $M_{H_2^0} = 220$ GeV, $M_{H^\pm} = 350$ GeV, $\text{Re}(m_{12}) = 170$ GeV, and $\alpha_3 = \pi/3$. On the top left plot $\tan \beta = 1.5$, top right: $\tan \beta = 2$, down left: $\tan \beta = 3$, and down right: $\tan \beta = 4.5$.

$\alpha_2 \approx 0$ and $\alpha_1 \approx \pi/3$ (yellow color). The position of this region shifts to the right for larger values of $\tan \beta$. The coupling $\mathcal{C}(H_1^0 H^\pm W^\mp)$ is complex. Therefore, the condition $\mathcal{C}(H_1^0 H^\pm W^\mp) \rightarrow 0$ also implies that its imaginary part $R_{13} \rightarrow 0$, which furthermore means that H_1^0 is dominated by its CP-even component.

This can be seen also from the sum rule given by eq. (2.18), which tell us that if $|\mathcal{C}(H_1^0 H^\pm W^\mp)|^2 \rightarrow 0$ then $\mathcal{C}(H_1^0 WW)^2 \rightarrow 1$ and H_1^0 , which has a maximal coupling to a W pair, is dominated by its CP-even component. According to our definitions of the CPV asymmetries in section 3.2, when $|\mathcal{C}(H_1^0 H^\pm W^\mp)|^2 \rightarrow 0$, the tree-level width $\Gamma^{\text{tree}}(H^\pm \rightarrow$

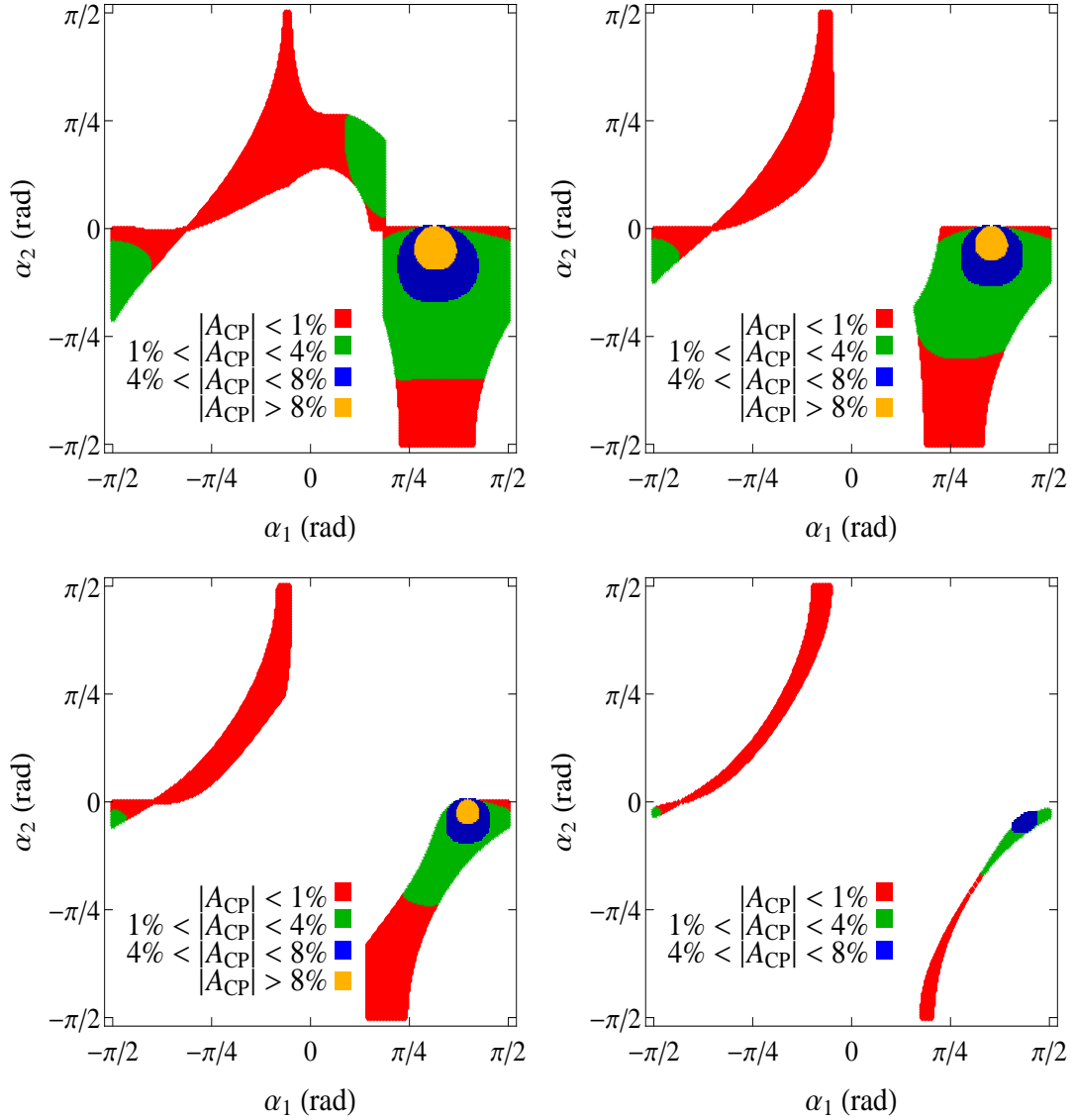


Figure 11. The allowed parameter regions in the (α_1, α_2) plan in the C2HDM together with the absolute value of the CPV asymmetry $A_{D,WH_1^0}^{CP}$. The other parameters are the same as for figure 10.

$W^\pm H_1^0 \rightarrow 0$ and consequently the CPV asymmetry will increase considerably. However, the large rate asymmetry we would obtain in this case, would go together with a small BR of the $H^\pm \rightarrow W^\pm H_1^0$ decay.

In figure 12 we show the BR of $H^\pm \rightarrow W^\pm H_1^0$ as a function of α_1 for various values of $\tan \beta$ and the other parameters fixed as in figure 10. It can be seen in the plots that in some cases the BR of $H^\pm \rightarrow W^\pm H_1^0$ can be larger than 80% together with a CPV asymmetry of a few percent.

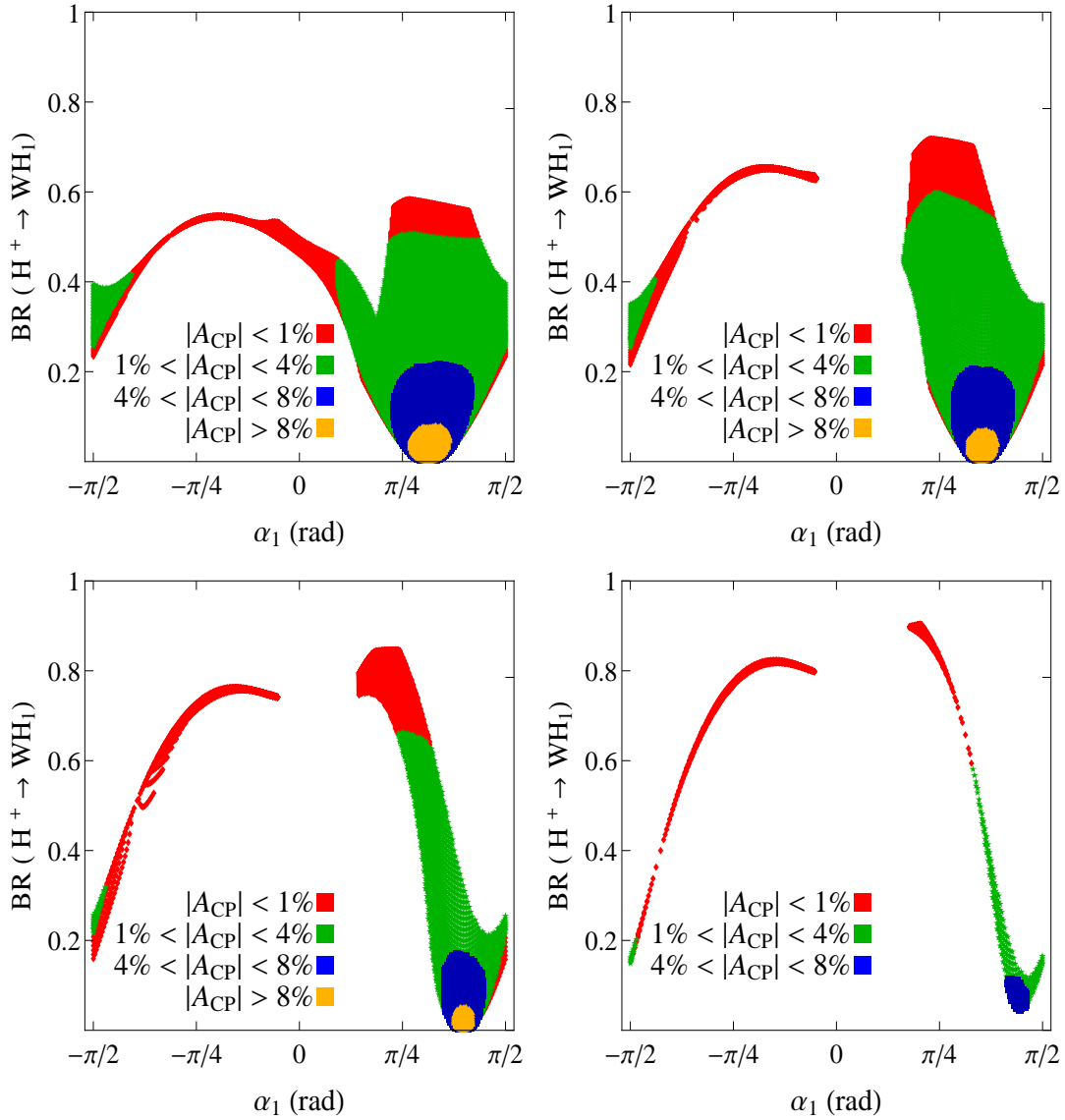


Figure 12. The $\text{BR}(H^+ \rightarrow W^+ H_1^0)$ as a function of α_1 with α_2 in the allowed parameter range. The other parameters are the same as for figure 10.

4.3 CP violation in H^\pm -production

We also study the CPV asymmetry A_P^{CP} , given by eq. (3.5), for charged Higgs production (3.2) at the LHC with $\sqrt{s} = 14$ TeV. For a direct comparison with the results of section 4.2, in figure 13 we present the asymmetry A_P^{CP} as a function of the charged Higgs mass M_{H^\pm} for the same parameter set as used for figure 7. One can see that here the asymmetry is of the same order of magnitude or smaller than in the $H^\pm \rightarrow tb$. The absolute value increases with $\tan\beta$, and can go up to 2% for $\tan\beta = 4$ and $M_{H^\pm} = 400$ GeV. But in contrast to the $H^\pm \rightarrow tb$ decay the production asymmetry is negative. Therefore, the total asymmetry $A_P^{CP} + A_{D,tb}^{CP}$ is very small. However, A_P^{CP} has the same sign like $A_{D,WH_{1,2}^0}^{CP}$ and

according to eq. (3.7) this will increase the total asymmetry in these bosonic modes.

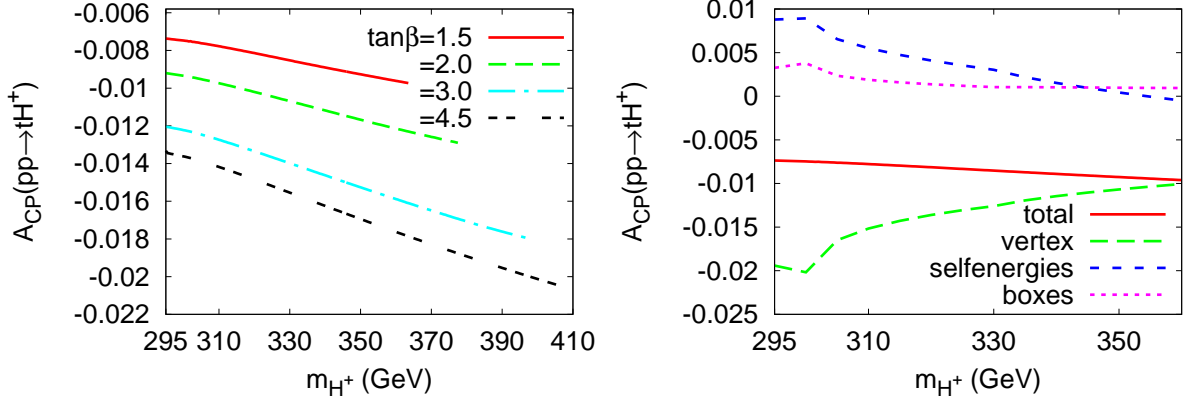


Figure 13. CPV asymmetry A_P^{CP} (3.5); Left: as a function of charged Higgs mass for four values of $\tan\beta$ and the other parameters are as in figure 7: $M_{H_1^0} = 120$ GeV, $M_{H_2^0} = 220$ GeV, $\text{Re}(m_{12}) = 170$ GeV, $\alpha_1 = 0.8$, $\alpha_2 = -0.9$ and $\alpha_3 = \pi/3$; Right: vertex, selfenergy and box contributions to A_P^{CP} as a function of M_{H^+} for $\tan\beta = 1.5$.

In figure 13 we show the vertex, selfenergy and box contributions to A_P^{CP} for $\tan\beta = 1.5$. The vertex contribution is negative and dominating, especially for smaller masses of the charged Higgs. The selfenergies and box contributions are both positive, but their sum partially cancels with the contributions of the vertex diagrams.

In figure 14 we show a scan over the angles α_1 and α_2 , together with the absolute value of the asymmetry A_P^{CP} , as for the decays in the previous section, see figure 10 and figure 11. The plots are very similar in size and the asymmetry can reach $\sim 2\%$.

In order to have a better overview on the CPV asymmetry in a larger parameter space and having in mind that the integration over the PDFs slows down the calculation considerably, we perform a numerical scan over the C2HDM parameters (2.13) using Grid computing:

$$\begin{aligned}
M_{H_1^0} &= 115 \div 125 \text{ GeV, with step size 5 GeV,} \\
M_{H_2^0} &= 150 \div 400 \text{ GeV, with step size 50 GeV,} \\
M_{H^+} &= 300 \div 550 \text{ GeV, with step size 25 GeV,} \\
\text{Re}(m_{12}) &= 10 \div 460, \text{ with step size 50,} \\
\tan\beta &= 1 \div 8, \text{ with step size 1,} \\
\alpha_1 &= \pi/2 \div \pi/2, \text{ with step size } \pi/9, \\
\alpha_2 &= \pi/2 \div \pi/2, \text{ with step size } \pi/9, \\
\alpha_3 &= 0 \div \pi/2, \text{ with step size } \pi/9,
\end{aligned} \tag{4.6}$$

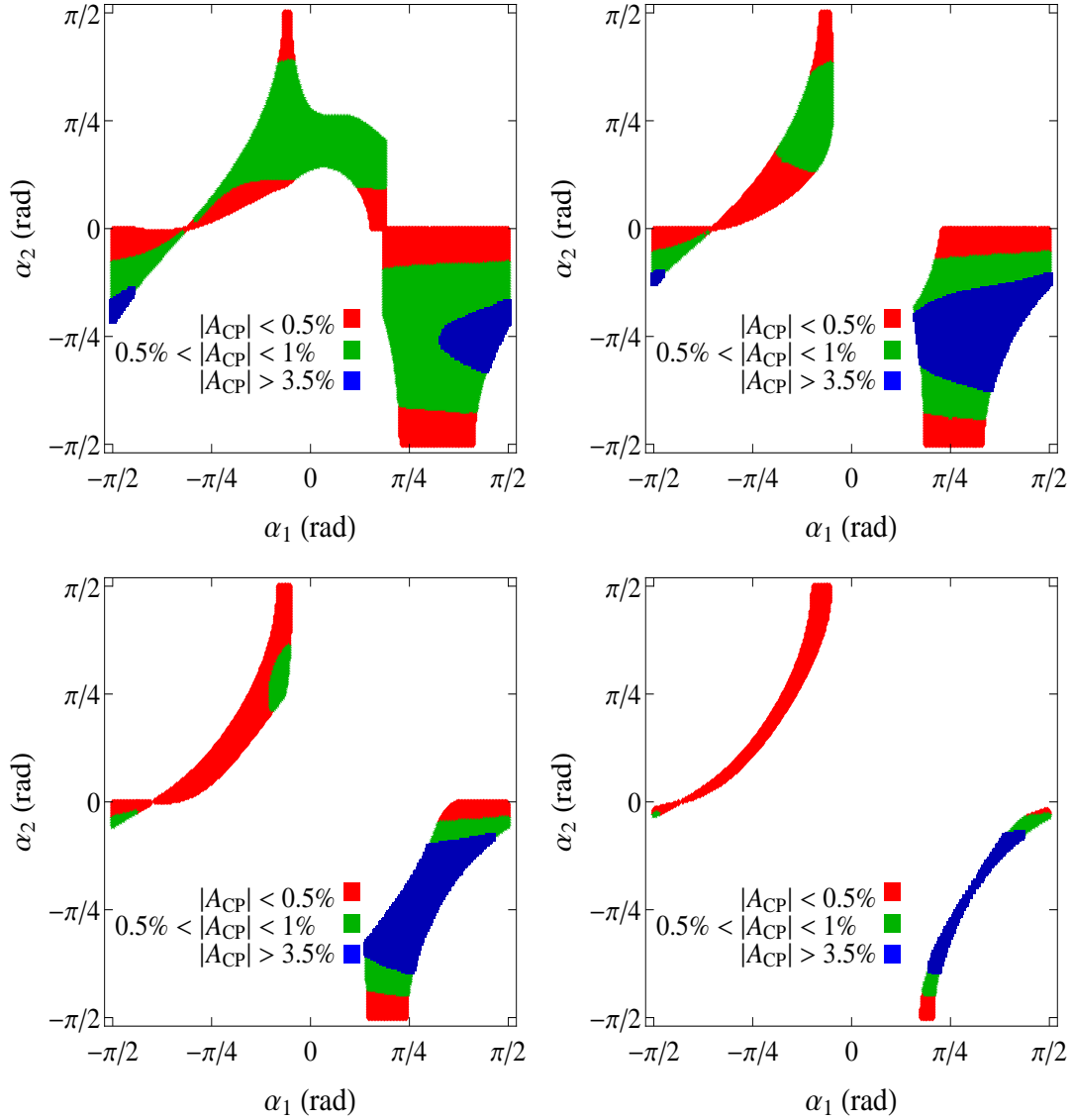


Figure 14. The allowed parameter regions in the (α_1, α_2) plan in the C2HDM together with the absolute value of the CPV asymmetry A_P^{CP} . The other parameters are the same as in figure 10.

The total number of the scanned parameter points is quite large: 6415200. After having applied the theoretical and experimental constraints, see section 2.5 and section 4.1, the allowed number of parameter points relegates to 67861, which is only 1% of the scanned parameter space.

The numerical results based on the parameter scan (4.6) show that in most of the cases the asymmetry is very small, practically zero. The non-zero asymmetry is distributed in two non-symmetric bunches - to the right (up to $\sim 2\%$) and to the left (down to $\sim -3\%$) from the zero. The non-symmetric structure of the distribution is due to the asymmetric $\Delta\rho$ constraints, see section 4.1. Furthermore, the results from the numerical scan (4.6)

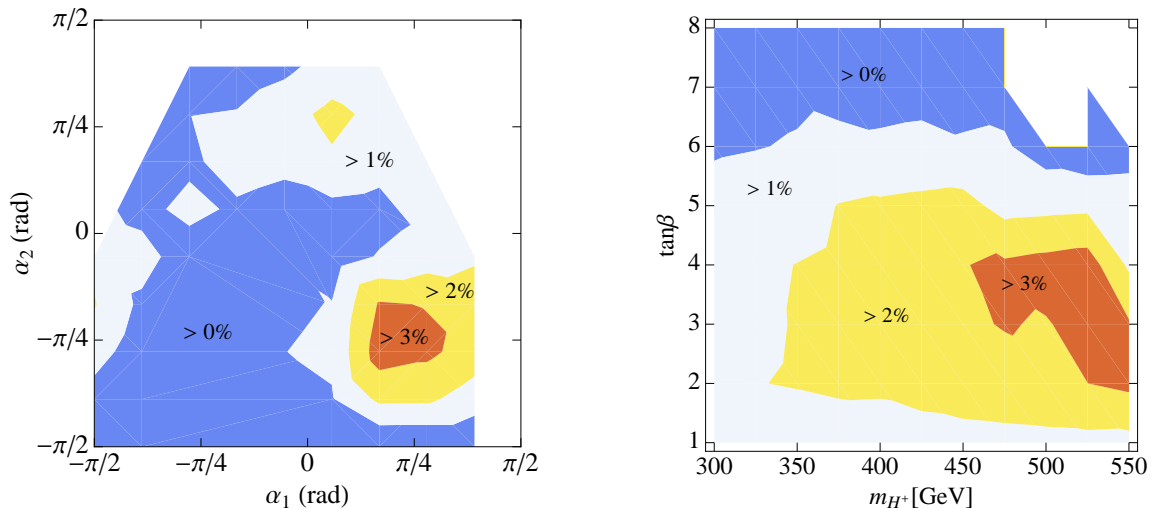


Figure 15. The maximal value of the asymmetry $|A_P^{CP}|$ as a function of α_1 and α_2 – left; and M_{H^+} and $\tan\beta$ – right, based on the parameter scan (4.6).

show that the CPV asymmetry A_P^{CP} can reach 3.5 % (negative) for single isolated points of the parameter space.

In figure 15 we show the maximal value of $|A_P^{CP}|$ as a function of α_1 and α_2 – left; and M_{H^+} and $\tan\beta$ – right, based on the parameter scan (4.6). One sees small regions where the asymmetry can go up to $\sim 3\%$. These are roughly: $(\alpha_1, -\alpha_2) \in (\pi/6 \div \pi/3)$ and relatively large M_{H^+} and $\tan\beta$: $M_{H^+} \in (460 \div 550)$ and $\tan\beta \in (2 \div 4)$. However, our experience showed that making a plot in such region is a question of fine-tuning of the parameters due to the severe theoretical constraints (see section 2.5), which often cut the parameter space into unconnected subspaces.

4.4 CP violation in H^\pm -production and subsequent decays

Combining the production process (3.3) with the subsequent decay $H^\pm \rightarrow tb$, in [13] we have shown analytically that the charged Higgs selfenergy contributions to the total asymmetry from the production and the decay exactly cancel. Moreover, we have shown that in the MSSM the vertex contributions from the production and from the decay also partially cancel. Eventually, the main contribution in the total asymmetry comes from the MSSM box contributions to the production.

In this paper we study the same production process, but in the C2HDM. The selfenergy cancellations observed in [13] are not model dependent and we expect them to occur again. In figure 16 we show the asymmetry A_{tb}^{CP} as a function of the charged Higgs mass. One sees that the total asymmetry is of an order of magnitude smaller in comparison to the individual decay and production asymmetries. The cancellations are easily traced back comparing the selfenergy and vertex contributions in figure 7 and figure 13, which are of the same magnitude, but with opposite signs. However, no such cancellations occur in the bosonic modes: $H^\pm \rightarrow W^\pm H_{1,2}^0$. In figure 17 we show the asymmetries $A_{WH_1}^{CP}$ and $A_{WH_2}^{CP}$

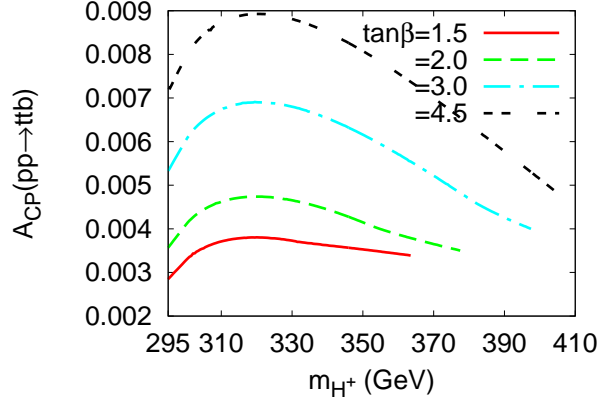


Figure 16. CPV asymmetry A_{tb}^{CP} (3.6) as a function of the charged Higgs mass for four values of $\tan \beta$ and the other parameters are as in figure 7: $M_{H_1^0} = 120$ GeV, $M_{H_2^0} = 220$ GeV, $\text{Re}(m_{12}) = 170$ GeV, $\alpha_1 = 0.8$, $\alpha_2 = -0.9$ and $\alpha_3 = \pi/3$.

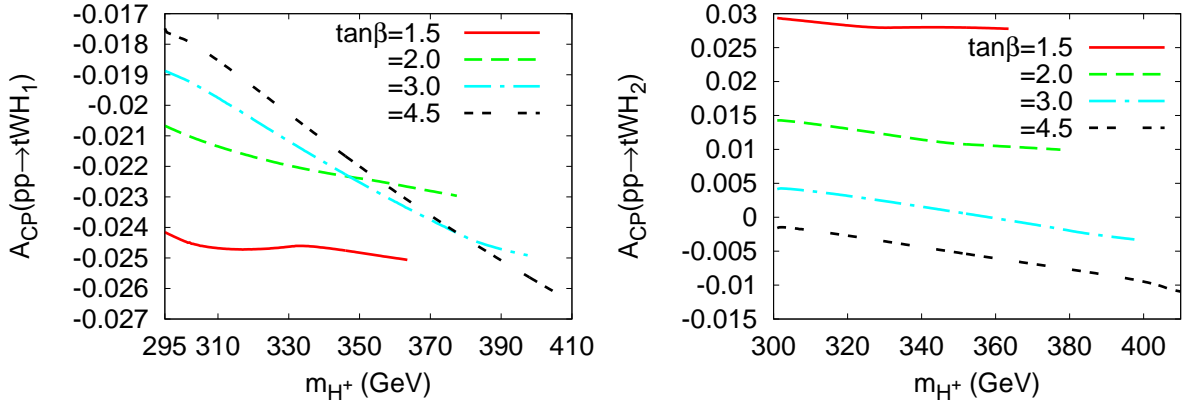


Figure 17. CPV asymmetries $A_{WH_1}^{CP}$ and $A_{WH_2}^{CP}$ (3.6) as functions of M_{H^+} for four values of $\tan \beta$. The other parameters are: $m_{H_1^0} = 120$ GeV, $m_{H_2^0} = 220$ GeV, $m_{12} = 170$ GeV, $\alpha_1 = 0.8$, $\alpha_2 = -0.9$, and $\alpha_3 = \pi/3$.

(3.6) as functions of M_{H^+} for four values of $\tan \beta$. As one can see, here the effect is bigger and the asymmetry $A_{WH_1}^{CP}$ can reach up to 2.5% (negative), while the asymmetry $A_{WH_2}^{CP}$ can go up to 3% (positive).

In the analogous study performed in the MSSM [13] the main contribution for the case with the decay $H^\pm \rightarrow tb$ is due to box graphs with gluino exchange which involves the strong coupling constant. This asymmetry reaches its largest value of $\sim -12\%$ for $m_{H^+} \sim 550$ GeV with a branching ratio $\text{BR}(H^+ \rightarrow t\bar{b}) \sim 20\%$.

In contrast to [13], in the present study the asymmetries are due to the exchange of neutral Higgs bosons and therefore of electroweak nature. In the tb mode the asymmetry always remains below $\sim 1\%$ with $\text{BR}(H^+ \rightarrow t\bar{b}) \sim 50\%$ for $m_{H^+} \sim 350$ GeV. In the $W^\pm H_1$

mode it can reach 2.5% for $m_{H^+} \sim 350$ GeV with $\text{BR}(H^+ \rightarrow W^\pm H_1)$ up to $\sim 45\%$.

The production rate of H^+ at the LHC for $m_{H^+} = 350$ GeV and $\tan \beta = 1.5$ is ~ 450 fb (including a K-factor from QCD of 1.3, see [64]). Assuming a branching ratio of 50% and an integrated luminosity of 200 fb^{-1} we get $N \sim 45000$ and $\sqrt{N} \simeq 212$. Furthermore, assuming $A^{CP} \sim 0.02$, the statistical significance $\sqrt{N} A_{tb}^{CP} \sim 4.2$. However, in a realistic study the actual signal production rate will be most likely reduced. Moreover, the total background rate for charged Higgs production at the LHC is quite large [64]. The obtained statistical significance might be too low for a clear observation in the first stage of the LHC and therefore an upgrade of its luminosity would be necessary to await.

5 Conclusions

In the type II complex 2HDM with softly broken Z_2 symmetry, the non-zero and complex m_{12}^2 parameter of the tree-level Higgs potential gives rise to CP violation in the production process $pp \rightarrow H^\pm t + X$, and in the dominant decay modes of H^\pm to tb , and to WH_i , $i=1,2$. We have calculated the corresponding CP violating rate asymmetries at one-loop level both in the production and in the decays, as well as in the combined processes. A detailed numerical analysis has been performed. The dependences of the asymmetries on the C2HDM parameters are studied taking into account the theoretical constraints, experimental lower bound on the charged Higgs mass from $B \rightarrow X_s \gamma$ and the constraint on the ρ parameter.

The calculations have been performed with the help of the packages FeynArts and FormCalc. For that purpose, a new model file for FeynArts has been created and corresponding fortran drivers for FormCalc have been written.

In the allowed parameter space of the C2HDM parameters, which is severely constrained by vacuum stability, perturbativity, unitarity, lower charged Higgs mass bound and $\Delta\rho$, the studied CP violating asymmetries cannot be greater than $\sim 3\%$. This is in contrast with a similar study performed within the MSSM [13]. There the CPV asymmetries can be larger by an order of magnitude. However, after having taken into account the relevant branching ratios and cross sections, the measurability of the studied CPV asymmetries in the C2HDM and in the MSSM at the LHC has roughly the same statistical significance, which is maybe not big enough for a clear observation at the LHC. At the SLHC with a design luminosity bigger by a factor of ~ 10 , such a measurement would be worth of being performed.

A The $\Delta\rho$ constraint

The ρ parameter is defined by the ratio of the neutral and charged currents at vanishing momentum transfer. In the C2HDM, at tree level $\rho = m_W^2/(c_W^2 m_Z^2) = 1$ which is in perfect agreement with the experimentally measured value. This relation may be spoiled by radiative corrections if they are large.

For the extra contributions $\Delta\rho$ to the ρ parameter from the additional scalars Higgses in the C2HDM, we have implemented in our code the expression given in [30] in terms of physical masses and elements R_{jk} of the rotation matrix (2.8). The analytic expression for $\Delta\rho$ can be split into two contributions:

i) Higgs–Higgs contribution (HH):²

$$A_{WW}^{HH}(0) - \cos^2 \theta_W A_{ZZ}^{HH}(0) = \frac{g^2}{64\pi^2} \sum_j \left[\{[\sin \beta R_{j1} - \cos \beta R_{j2}]^2 + R_{j3}^2\} F_{\Delta\rho}(M_{H^\pm}^2, M_j^2) \right. \\ \left. - \sum_{k>j} [(\sin \beta R_{j1} - \cos \beta R_{j2}) R_{k3} - (\sin \beta R_{k1} - \cos \beta R_{k2}) R_{j3}]^2 F_{\Delta\rho}(M_j^2, M_k^2) \right], \quad (\text{A.1})$$

with

$$F_{\Delta\rho}(m_1^2, m_2^2) = \frac{1}{2}(m_1^2 + m_2^2) - \frac{m_1^2 m_2^2}{m_1^2 - m_2^2} \log \frac{m_1^2}{m_2^2}. \quad (\text{A.2})$$

ii) Higgs–ghost contribution (HG):

$$A_{WW}^{HG}(0) - \cos^2 \theta_W A_{ZZ}^{HG}(0) = \frac{g^2}{64\pi^2} \left[\sum_j [\cos \beta R_{j1} + \sin \beta R_{j2}]^2 \times \right. \\ \left. \times \left(3F_{\Delta\rho}(M_Z^2, M_j^2) - 3F_{\Delta\rho}(M_W^2, M_j^2) \right) + 3F_{\Delta\rho}(M_W^2, M_0^2) - 3F_{\Delta\rho}(M_Z^2, M_0^2) \right]. \quad (\text{A.3})$$

From this contribution one has to subtract the SM Higgs contribution of a mass M_0 [30]. The choice of M_0 is usually consistent with the fit analysis. As a default value we take $M_0 = 120$ GeV.

B Expressions for λ_i

In order to work with the parameter set (2.13), we need the explicit relations between the parameters of the Higgs potential and the physical Higgs masses and rotation angles. It is straightforward to derive the λ_i , $i = 1, 2, 3, 4, 5$ as functions of our input parameters (2.13)

²The relevant couplings are given explicitly in appendix B of [30].

[29]:

$$\begin{aligned}
\lambda_1 &= \frac{1}{c_\beta^2 v^2} [c_1^2 c_2^2 M_{H_1^0}^2 + (c_1 s_2 s_3 + s_1 c_3)^2 M_{H_2^0}^2 + (c_1 s_2 c_3 - s_1 s_3)^2 M_{H_3^0}^2 - s_\beta^2 \mu^2], \\
\lambda_2 &= \frac{1}{s_\beta^2 v^2} [s_1^2 c_2^2 M_{H_1^0}^2 + (c_1 c_3 - s_1 s_2 s_3)^2 M_{H_2^0}^2 + (c_1 s_3 + s_1 s_2 c_3)^2 M_{H_3^0}^2 - c_\beta^2 \mu^2], \\
\lambda_3 &= \frac{1}{s_\beta c_\beta v^2} \{c_1 s_1 [c_2^2 M_{H_1^0}^2 + (s_2^2 s_3^2 - c_3^2) M_{H_2^0}^2 + (s_2^2 c_3^2 - s_3^2) M_{H_3^0}^2] \\
&\quad + s_2 c_3 s_3 (c_1^2 - s_1^2) (M_{H_3^0}^2 - M_{H_2^0}^2)\} + \frac{1}{v^2} [2M_{H^+}^2 - \mu^2], \\
\lambda_4 &= \frac{1}{v^2} [s_2^2 M_{H_1^0}^2 + c_2^2 s_3^2 M_{H_2^0}^2 + c_2^2 c_3^2 M_{H_3^0}^2 + \mu^2 - 2M_{H^+}^2], \\
\text{Re}(\lambda_5) &= \frac{1}{v^2} [-s_2^2 M_{H_1^0}^2 - c_2^2 s_3^2 M_{H_2^0}^2 - c_2^2 c_3^2 M_{H_3^0}^2 + \mu^2], \\
\text{Im}(\lambda_5) &= -\frac{1}{c_\beta s_\beta v^2} \{c_\beta [c_1 c_2 s_2 M_{H_1^0}^2 - c_2 s_3 (c_1 s_2 s_3 + s_1 c_3) M_{H_2^0}^2 \\
&\quad + c_2 c_3 (s_1 s_3 - c_1 s_2 c_3) M_{H_3^0}^2] + s_\beta [s_1 c_2 s_2 M_{H_1^0}^2 + c_2 s_3 (c_1 c_3 - s_1 s_2 s_3) M_{H_2^0}^2 \\
&\quad - c_2 c_3 (c_1 s_3 + s_1 s_2 c_3) M_{H_3^0}^2]\}, \tag{B.1}
\end{aligned}$$

with $s_\beta = \sin \beta$, $c_\beta = \cos \beta$ and μ is given by eq. (4.2).

The expressions (B.1) are implemented in our numerical code. Note that there are limits of non-CPV in the C2HDM [29], corresponding to the following values of the α -parameters:

$$\begin{aligned}
\alpha_2 &= \pm \pi/2, \\
\alpha_3 &= \pm \pi/2, \\
\alpha_2 &= \alpha_3 = 0. \tag{B.2}
\end{aligned}$$

At these limits, the elements R_{13} , R_{23} and R_{33} of the mixing matrix (2.8) vanish and the expression (2.15) becomes unstable. As this case is a subject of a different model convention, namely it is already the CP conserving 2HDM, our numerical code would produce an error message and interrupt the evaluation.

C Interaction Lagrangian

For our calculations we have used the following part of the C2HDM Lagrangian:

C.0.1 Interactions of two quarks with a gluon

$$\mathcal{L}_{\bar{q}qg} = -g_s T_{kl}^\alpha G_\mu^\alpha \bar{q}_k \gamma^\mu q_l, \quad k, l = 1, 2, 3, \quad \alpha = 1, \dots, 8, \quad q = t, b, \tag{C.1}$$

where $T^\alpha/2$ are the Gell-Mann matrices and g_s is the SU(3) strong coupling constant.

C.0.2 Yukawa interactions of the neutral and the charged Higgses

$$\begin{aligned}
\mathcal{L}_{\bar{t}tH_j^0} &= \bar{t}(h_{t,j}^L P_L + h_{t,j}^R P_R)tH_j^0, \quad j = 1, 2, 3, \\
h_{t,j}^L &= -\frac{1}{\sqrt{2}}(R_{j2} + ic_\beta R_{j3})h_t, \\
h_{t,j}^R &= -\frac{1}{\sqrt{2}}(R_{j2} - ic_\beta R_{j3})h_t, \quad h_t = \frac{gm_t}{\sqrt{2}m_W s_\beta}, \\
\mathcal{L}_{\bar{b}bH_j^0} &= \bar{b}(h_{b,j}^L P_L + h_{b,j}^R P_R)bH_j^0, \quad j = 1, 2, 3, \\
h_{b,j}^L &= -\frac{1}{\sqrt{2}}(R_{j1} + is_\beta R_{j3})h_b, \\
h_{b,j}^R &= -\frac{1}{\sqrt{2}}(R_{j1} - is_\beta R_{j3})h_b, \quad h_b = \frac{gm_b}{\sqrt{2}m_W c_\beta}, \\
\mathcal{L}_{tbH^\pm} &= \bar{t}(y_t P_L + y_b P_R)bH^+ + \bar{b}(y_b P_L + y_t P_R)tH^-, \\
y_t &= h_t c_\beta, \quad y_b = h_b s_\beta,
\end{aligned} \tag{C.2}$$

with $s_\beta = \sin \beta$ and $c_\beta = \cos \beta$; $P_L = (1 - \gamma_5)/2$ and $P_R = (1 + \gamma_5)/2$ denote the left and right projection operators, respectively, R_{jk} with $j, k = 1, 2, 3$ are the elements of the mixing matrix \mathcal{R} , see eq. (2.8).

C.0.3 Two quarks-W and two quarks-ghost interactions

$$\begin{aligned}
\mathcal{L}_{tbW^\pm} &= -\frac{g}{\sqrt{2}}(\bar{t}\gamma^\mu P_L bW_\mu^+ + \bar{b}\gamma^\mu P_L tW_\mu^-); \\
\mathcal{L}_{tbG^\pm} &= \bar{t}(\tilde{y}_t P_L + \tilde{y}_b P_R)bG^+ + \bar{b}(\tilde{y}_b P_L + \tilde{y}_t P_R)tG^-, \\
\tilde{y}_t &= \frac{gm_t}{\sqrt{2}m_W}, \quad \tilde{y}_b = \frac{gm_b}{\sqrt{2}m_W}.
\end{aligned} \tag{C.3}$$

C.0.4 Triple scalar interactions with neutral and charged Higgses

$$\begin{aligned}
\mathcal{L}_{H_j^0 H^+ H^-} &= -\frac{2m_W}{g}(f_{H^0 H^+ H^-})_j H_j^0 H^+ H^-, \quad j = 1, 2, 3, \\
(f_{H^0 H^+ H^-})_j &= c_\beta[s_\beta^2(\lambda_1 - \lambda_4 - \text{Re}(\lambda_5)) + c_\beta^2 \lambda_3]R_{j1} + \\
&\quad s_\beta[c_\beta^2(\lambda_2 - \lambda_4 - \text{Re}(\lambda_5)) + s_\beta^2 \lambda_3]R_{j2} + s_\beta c_\beta \text{Im}(\lambda_5)R_{j3}.
\end{aligned} \tag{C.4}$$

C.0.5 Neutral Higgs-charged Higgs-W and neutral Higgs-charged Higgs-ghost interactions

$$\begin{aligned}
\mathcal{L}_{H_j^0 H^+ W^-} &= \frac{ig}{2}(s_\beta R_{j1} - c_\beta R_{j2} + iR_{j3})[H_j^0 \overset{\leftrightarrow}{\partial}^\mu H^+ W^{\mu-} - H_j^0 \overset{\leftrightarrow}{\partial}^\mu H^- W^{\mu+}], \\
&\quad j = 1, 2, 3, \\
\mathcal{L}_{H_j^0 H^+ G^-} &= \frac{m_W}{g}(f_{H^0 H^+ G^-})_j H_j^0 H^+ G^- + \text{h.c.}, \quad j = 1, 2, 3, \\
(f_{H^0 H^+ G^-})_j &= s_\beta[s_\beta^2(\lambda_4 + \text{Re}(\lambda_5)) + c_\beta^2(2\lambda_1 - \lambda_3 - \lambda_{345}) - i\text{Im}(\lambda_5)]R_{j1} + \\
&\quad c_\beta[-c_\beta^2(\lambda_4 + \text{Re}(\lambda_5)) - s_\beta^2(2\lambda_2 - \lambda_3 - \lambda_{345}) - i\text{Im}(\lambda_5)]R_{j2} + \\
&\quad [i(\lambda_4 - \text{Re}(\lambda_5)) + (c_\beta^2 - s_\beta^2)\text{Im}(\lambda_5)]R_{j3}, \\
\lambda_{345} &= \lambda_3 + \lambda_4 + \text{Re}(\lambda_5), \quad j = 1, 2, 3.
\end{aligned} \tag{C.5}$$

C.0.6 Interactions of a neutral Higgs with W-W, W-ghost and ghost-ghost

$$\begin{aligned}
\mathcal{L}_{H_j^0 W^+ W^-} &= g m_W (c_\beta R_{j1} + s_\beta R_{j2}) H_j^0 W_\mu^+ W^{\mu-}, \quad j = 1, 2, 3, \\
\mathcal{L}_{H_j^0 G^+ W^-} &= -\frac{ig}{2} (c_\beta R_{j1} + s_\beta R_{j2}) [H_j^0 \overset{\leftrightarrow}{\partial}^\mu G^+ W^{\mu-} - H_j^0 \overset{\leftrightarrow}{\partial}^\mu G^- W^{\mu+}], \quad j = 1, 2, 3, \\
\mathcal{L}_{H_j^0 G^+ G^-} &= -\frac{2m_W}{g} [c_\beta (c_\beta^2 \lambda_1 + s_\beta^2 \lambda_{345}) R_{j1} + \\
&\quad s_\beta (s_\beta^2 \lambda_2 + c_\beta^2 \lambda_{345}) R_{j2} - s_\beta c_\beta \text{Im}(\lambda_5) R_{j3}] H_j^0 G^+ G^-, \quad j = 1, 2, 3. \quad (\text{C.6})
\end{aligned}$$

D Implementation of the complex 2HDM into FeynArts and FormCalc

At present, there are several software packages for deriving Feynman rules and doing calculations of particle processes on the market e.g. [16, 65, 67]. For the purpose of our work it is convenient to use the FA package. Up to now the FA package does not include a model file for the 2HDM with CPV. In the following sections we describe how we have implemented the new model file for calculations in the C2HDM into FA, and how we have extended the corresponding FC fortran drivers.

D.1 FeynArts model file for the C2HDM

At the moment, the diagram generator FA recognizes three generic particle physics models: the SM, the MSSM and the 2HDM [16]. The information about the physics properties of each model (fields, their propagators and their couplings) is collected in the corresponding model file. The model files for these three models exist in two different varieties: based only on the electroweak subset or including in addition quantum chromodynamics: `SM(QCD).mod`, `MSSM(QCD).mod`, `THDM(QCD).mod`. All couplings are expressed in terms of the parameters of the relevant Lagrangian.

The 2HDM model implemented in FA is based on the Higgs potential (2.1), but with $m_{12}^2 = \lambda_6 = \lambda_7 = 0$ and all other parameters are real. The latter constraints refer to a model with the particle content of the SM, but a physical Higgs sector analogous to the one of the MSSM, see e.g. [68]. Usually, this is the most commonly used version studied in literature, also called the CP-conserving 2HDM due to absence of complex parameters. (Note that there exist another public software package for calculations in the CP-conserving 2HDM [65].) In order to generalize the existing 2HDM model file for the general complex case, which is described by the Higgs potential (2.1), one should recalculate the couplings in terms of the full set of parameters in eq. (2.1).³ The new FA model file `CTHDM.mod` consists of 270 couplings, which includes all Higgs interactions:

- Higgs-vector boson interactions extracted from the covariant derivatives (2.16)
- Triple and quartic Higgs self-interactions from the scalar potential (2.1)
- Higgs interactions with Fadeev-Popov ghosts

³In this case the fields and their propagators are not affected.

- Yukawa interactions⁴

Some of them are obtained explicitly e.g. in [29, 69]. The rest of the couplings needed to complete the model file are not concerned and we have taken them from the already existing model file `THDM.mod`. These are: vector boson self-interactions, fermion-vector interactions, and with QCD couplings: gluon self-interactions, gluon-ghost and gluon-quark interactions. The model file can be used independently for diagram generation in the general complex case of the 2HDM and it is not necessarily related to further calculations. There is a rule included for a switch to the case $\lambda_6 = \lambda_7 = 0$, which describes the 2HDM with a softly broken Z_2 symmetry (2.10). In order to go back to the CP-conserving case one must also set m_{12}^2 to zero and consider λ_5 as a real parameter. The complete `CTHDM.mod` is too lengthy to be printed explicitly in this note. It can be found and downloaded from the FA website: www.feynarts.de.

D.2 FormCalc drivers for the C2HDM

After the diagram generation with the new FA model file `CTHDM.mod` FC calculates the squared matrix elements with the help of Form [71] and the resulting expressions are translated into Fortran for the further numerical evaluation. For consistency, the Fortran drivers necessary for the initialization of the model have to be extended to include the new set of parameters of the Higgs potential, the relations between them and the constraints on them. We would like to note that in spite of the fact that the new FA model file is written for the most general complex case with scalar potential (2.1), the extension of the FC fortran drivers is made only for the case of a softly broken Z_2 symmetry of the 2HDM Lagrangian, described by the scalar potential (2.10). The existing initialization file `model.thdm.F` is replaced by the new file `model.cthdm.F`, which defines all parameters of the potential (2.10), the theoretical and experimental constraints on them. Also the set of input parameters for the numerical evaluation in the C2HDM is defined therein. All implemented expressions are listed and discussed in the present paper.

Since the triple and the quartic scalar couplings have complicated and lengthy expressions, during the calculation of a given process they are replaced by generic couplings named `cS(i,j,k)` and `qS(i,j,k,l)`. Furthermore, all triple and quartic scalar couplings are evaluated in the `model.cthdm.F` file.

D.2.1 Inputs

Based on the case with a softly broken Z_2 symmetry of the 2HDM Lagrangian described by the scalar potential (2.10) we work with the following set of input parameters:

- $M_{h0} = M_{H_1^0}$ – mass of H_1^0
- $M_{HH} = M_{H_2^0}$ – mass of H_2^0
- $M_{Hp} = M_{H^\pm}$ – mass of the charged Higgs

⁴Note that here we assume one Higgs doublet to couple with only up-type fermions and the other one-only with down-type fermions or the so called 2HDM type II.

- $\text{TB} = v_1/v_2$ – the ratio of the VEVs
- $\text{rm12} = \text{Re}(m_{12})$ – real part of the m_{12} parameter of the Higgs potential
- $\text{alp1} = \alpha_1$ – mixing angle
- $\text{alp2} = \alpha_2$ – mixing angle
- $\text{alp3} = \alpha_3$ – mixing angle
- $\text{rm0} = M_0 = 120 \text{ GeV}$: reference point to subtract the SM Higgs contribution from $\Delta\rho$, see section A

Once the input parameters are initiated in `run.F`, in `model_cthdm.F` the mass of the heaviest neutral Higgs $M_{H_3^0}$ is calculated by using eq. (2.15). Then $M_{H_3^0}$ has to satisfy the following conditions:

- $M_{H_3^0}^2 > 0$, which means that H_3 is not a tachyonic mode;
- $M_{H_1^0} \leq M_{H_2^0} \leq M_{H_3^0}$, see section 2.1.

When an allowed value for $M_{H_3^0}$ is obtained, the code proceeds with the evaluation of the λ_i as given in appendix B. Finally, the triple and the quartic scalar couplings are calculated in `model_cthdm.F`.

D.2.2 Constraints

The file `model_cthdm.F` contains the following constraints, see section 2.5 and section 4.1:

- Vacuum stability
- Perturbativity and unitarity
- $\Delta\rho$ constraint

All constraints can be switched on and off. In addition, the upper and the lower $\Delta\rho$ bounds can be modified easily.

Acknowledgments

The authors thank Dietrich Liko for his help in Grid computing and Walter Majerotto for useful comments. A. Arhrib and E. Christova thank E. Ginina and H. Eberl for the hospitality during their visits in Vienna. The authors acknowledge support from EU under the MRTN-CT-2006-035505 network programme. This work is supported by the "Fonds zur Förderung der wissenschaftlichen Forschung" (FWF) of Austria, projects No. P18959-N16 and I297-N16. The work of E. Christova and E. Ginina is supported by the Bulgarian National Science Foundation, grant 288/2008.

References

- [1] A. Riotto, *Theories of baryogenesis*, Lectures delivered at the Summer School in High Energy Physics and Cosmology, Trieste, Italy, June - July 1998, [arXiv:hep-ph/9807454].
- [2] A. D. Dolgov, *Baryogenesis, 30 Years after*, Lectures given at the 25th ITEP Winter School of Physics, Moscow, Russia, February 1997, [arXiv:hep-ph/9707419].
- [3] W. Bernreuther, *CP violation and baryogenesis*, *Lect. Notes Phys.* **591** (2002) 237, [arXiv:hep-ph/0205279].
- [4] G. C. Branco, L. Lavoura and J. P. Silva, *CP violation*, *Int. Ser. Monogr. Phys.* **103** (1999) 1.
- [5] J. F. Gunion and H. E. Haber, *Conditions for CP-violation in the general two-Higgs-doublet model*, *Phys. Rev. D* **72** (2005) 095002, [arXiv:hep-ph/0506227].
- [6] G. C. Branco, M. N. Rebelo and J. I. Silva-Marcos, *CP-odd invariants in models with several Higgs doublets*, *Phys. Lett. B* **614** (2005) 187, [arXiv:hep-ph/0502118].
- [7] M. Carena, J. R. Ellis, A. Pilaftsis and C. E. Wagner, *Renormalization-Group-Improved Effective Potential for the MSSM Higgs Sector with Explicit CP Violation*, *Nucl. Phys. B* **586** (2000) 92, [arXiv: hep-ph/0003180].
- [8] E. Christova, H. Eberl, W. Majerotto and S. Kraml, *CP violation in charged Higgs decays in the MSSM with complex parameters*, *Nucl. Phys. B* **639** (2002) 263 [Erratum-ibid. **647** (2002) 359], [arXiv:hep-ph/0205227].
- [9] E. Christova, H. Eberl, E. Ginina and W. Majerotto, *CP violation in charged Higgs decays in the MSSM*, *JHEP* **0702** (2007) 075, [arXiv:hep-ph/0612088].
- [10] E. Christova, E. Ginina and M. Stoilov, *Supersymmetry through CP violation in $H^\pm \rightarrow W^\pm h^0$* , *JHEP* **0311** (2003) 027, [arXiv:hep-ph/0307319].
- [11] W. Hollik, D. T. Nhung, *CP violating asymmetry in $H^\pm \rightarrow W^\pm h_1$ decays*, [arXiv:1008.2659, hep-ph].
- [12] T. N. Dao, W. Hollik and D. N. Le, *$W^\mp H^\pm$ production and CPV asymmetry at the LHC*, [arXiv:1011.4820, hep-ph].
- [13] E. Christova, H. Eberl, E. Ginina and W. Majerotto, *CP violation in $H^\pm t$ production at the LHC*, *Phys. Rev. D* **79** (2009) 096005, [arXiv:0812.4392, hep-ph].
- [14] E. Ginina, E. Christova and H. Eberl, *CP violation in associated production of charged Higgs boson and top quark at the LHC*, *PoS CHARGED2008* (2008) 013, [arXiv:0812.1129, hep-ph].
- [15] E. Christova, H. Eberl and E. Ginina, *Charged Higgs production at the LHC and CPV asymmetries*, *AIP Conf. Proc.* **1200** (2010) 522, [arXiv:0912.3156, hep-ph].
- [16] T. Hahn, *Generating Feynman Diagrams and Amplitudes with FeynArts 3*, *Comput. Phys. Commun.* **140** (2001) 418, [arXiv:hep-ph/0012260].
- [17] J. Küblbeck, M. Böhm, A. Denner, *Feyn arts computer-algebraic generation of Feynman graphs and amplitudes*, *Comput. Phys. Commun.* **60** (1990) 165.
- [18] T. Hahn and J. I. Illana, *Excursions into FeynArts and FormCalc*, *Nucl. Phys. Proc. Suppl.* **160** (2006) 101.
- [19] T. Hahn, M. Perez-Victoria, *Automatized One-Loop Calculations in 4 and D dimensions*, *Comput. Phys. Commun.* **118** (1999) 153, [arXiv:hep-ph/9807565].

- [20] J. F. Gunion, H. E. Haber, G. Kane, S. Dawson, *The Higgs Hunter's Guide*, Addison-Wesley Publishing Co, 1990.
- [21] R. A. Diaz, *Phenomenological analysis of the two Higgs doublet model*, PhD Thesis, Universidad Nacional de Colombia, [arXiv:hep-ph/0212237].
- [22] W. S. Hou, *Enhanced charged Higgs boson effects in $B^- \rightarrow \tau \text{ anti-neutrino}$, $\mu \text{ anti-neutrino}$ and $b \rightarrow \tau \text{ anti-neutrino} + X$* , *Phys. Rev. D* **48** (1993) 2342.
- [23] A. G. Akeroyd and F. Mahmoudi, *Constraints on charged Higgs bosons from $D(s)^\pm \rightarrow \mu^\pm \nu$ and $D(s)^\pm \rightarrow \tau^\pm \nu$* , *JHEP* **0904** (2009) 121, [arXiv:0902.2393, hep-ph].
- [24] T. D. Lee, *A Theory of Spontaneous T Violation*, *Phys. Rev. D* **8** (1973) 1226.
- [25] G. C. Branco and M. N. Rebelo, *The Higgs Mass In A Model With Two Scalar Doublets And Spontaneous CP Violation*, *Phys. Lett. B* **160** (1985) 117.
- [26] S. Weinberg, *Gauge Theory Of CP Violation*, *Phys. Rev. Lett.* **37** (1976) 657.
- [27] J. Liu and L. Wolfenstein, *Spontaneous CP Violation In The $SU(2)_L \times U(1)_Y$ Model With Two Higgs Doublets*, *Nucl. Phys. B* **289** (1987) 1.
- [28] Ilya F. Ginzburg and Maria Krawczyk, *Symmetries of the THDM and CP violation*, *Phys. Rev. D* **72** (2005) 115013, [arXiv:hep-ph/0408011].
- [29] P. Osland, P. N. Pandita and L. Selbuz, *Trilinear Higgs couplings in the two Higgs doublet model with CP violation*, *Phys. Rev. D* **78** (2008) 015003, [arXiv:0802.0060, hep-ph].
- [30] A. W. El Kaffas, W. Khater, O. M. Ogreid and P. Osland, *Consistency of the Two Higgs Doublet Model and CP violation in top production at the LHC*, *Nucl. Phys. B* **775** (2007) 45, [arXiv:hep-ph/0605142].
- [31] S. L. Glashow and S. Weinberg, *Natural conservation laws for neutral currents*, *Phys. Rev. D* **15** (1977) 1958.
- [32] W. Khater, P. Osland, *CP violation in top quark production at the LHC and Two-Higgs-Doublet Models*, *Nucl. Phys. B* **661** (2003) 209, [arXiv:hep-ph/0302004].
- [33] B. Grzadkowski, P. Osland, *A natural Two-Higgs-Doublet Model*, [arXiv:0910.4068, hep-ph].
- [34] A. Wahab El Kaffas, P. Osland, O. M. Ogreid, *CPV, Stability and Unitarity of the THDM, Nonlin. Phenom. ComplexSyst.* **10** (2007) 347-357, [arXiv:hep-ph/0702097].
- [35] A. Wahab El Kaffas, P. Osland and O. M. Ogreid, *Constraining the Two-Higgs-Doublet-Model parameter space*, *Phys. Rev. D* **76** (2007) 095001, [arXiv:0706.2997, hep-ph].
- [36] R. M. Barnett, G. Senjanovic and D. Wyler, *Tracking Down Higgs Scalars With Enhanced Couplings*, *Phys. Rev. D* **30** (1984) 1529.
- [37] R. M. Barnett, G. Senjanovic, L. Wolfenstein and D. Wyler, *Implications Of A Light Higgs Scalar*, *Phys. Lett. B* **136** (1984) 191.
- [38] A. G. Akeroyd, *Non-minimal neutral Higgs bosons at LEP2*, *Phys. Lett. B* **377** (1996) 95, [arXiv:hep-ph/9603445].
- [39] M. Aoki, S. Kanemura, K. Tsumura and K. Yagyu, *Models of Yukawa interaction in the two Higgs doublet model, and their collider phenomenology*, *Phys. Rev. D* **80** (2009) 015017, [arXiv:0902.4665, hep-ph].
- [40] H. E. Logan and D. MacLennan, *Charged Higgs phenomenology in the lepton-specific two*

- Higgs doublet model*, *Phys. Rev. D* **79** (2009) 115022, [arXiv:0903.2246, hep-ph].
- [41] S. Su and B. Thomas, *The LHC Discovery Potential of a Leptophilic Higgs*, *Phys. Rev. D* **79** (2009) 095014, [arXiv:0903.0667, hep-ph].
 - [42] G. J. van Oldenborgh, *FF: A Package to evaluate one loop Feynman diagrams*, *Comput. Phys. Commun.* **66** (1991) 1.
 - [43] T. Hahn, *Loop Calculations with FeynArts, FormCalc, and LoopTools*, *Acta Phys. Polon. B* **30** (1999) 3469-3475, [arXiv:hep-ph/9910227].
 - [44] T. Hahn, *FeynArts User's Guide, FormCalc User's Guide and LoopTools User's Guide*, available at <http://www.feynarts.de>
 - [45] C. Amsler et al., [Particle Data Group], *Review of particle physics*, *Phys. Lett. B* **667** (2008) 1.
 - [46] Tevatron Electroweak Working Group and CDF Collaboration and D0 Collab, *Combination of CDF and D0 Results on the Mass of the Top Quark*, [arXiv:0903.2503, hep-ex].
 - [47] T. Hayashi, Y. Koide, M. Matsuda, M. Tanimoto, S. Wakaizumi, *Electric Dipole Moments of Neutron and Electron in Two-Higgs-Doublet Model with Maximal CP violation*, *Phys. Lett. B* **348** (1995) 489-495, [arXiv:hep-ph/9410413].
 - [48] A. W. El Kaffas, O. M. Ogreid, P. Osland, *Probing triple Higgs couplings of the Two Higgs Doublet Model at Linear Collider*, *Phys. Rev. D* **77** (2008) 115013, [arXiv:0802.0319, hep-ph].
 - [49] A. Arhrib, R. Benbrik, C.-W. Chiang, *Profile of Two-Higgs-Doublet-Model Parameter Space*, *Phys. Rev. D* **77** (2008) 115013, [arXiv:0802.0319, hep-ph].
 - [50] K. Nakamura et al., [Particle Data Group], *Review of Particle Physics*, *J. Phys. G* **37** (2010) 075021.
 - [51] R. Barate et al., [ALEPH, DELPHI, L3 and OPAL Collaborations, The LEP Working Group for Higgs Boson Searches], *Search for the standard model Higgs boson at LEP*, *Phys. Lett. B* **565** (2003) 61, [arXiv:hep-ex/0306033].
 - [52] S. Schael et al., [ALEPH, DELPHI, L3 and OPAL Collaborations, The LEP Working Group for Higgs Boson Searches], *Search for neutral MSSM Higgs bosons at LEP*, *Eur. Phys. J. C* **47** (2006) 547, [arXiv:hep-ex/0602042].
 - [53] A. Abulencia et al., [CDF Collaboration], *Search for charged Higgs bosons from top quark decays in $p\bar{p}$ collisions at $\sqrt{s} = 1.96$ TeV*, *Phys. Rev. Lett.* **96** (2006) 042003, [arXiv:hep-ex/0510065].
 - [54] V. M. Abazov et al., [D0 Collaboration], *Direct search for charged Higgs bosons in decays of top quarks*, *Phys. Rev. Lett.* **88** (2002) 151803, [arXiv:hep-ex/0102039].
 - [55] M. Ciuchini, G. Degrossi, P. Gambino and G. F. Giudice, *Next-to-leading QCD corrections to $B \rightarrow X/s$ gamma: Standard model and two-Higgs doublet model*, *Nucl. Phys. B* **527** (1998) 21, [arXiv:hep-ph/9710335].
 - [56] P. Ciafaloni, A. Romanino and A. Strumia, *Two-loop QCD corrections to charged-Higgs-mediated $b \rightarrow s$ gamma decay*, *Nucl. Phys. B* **524** (1998) 361, [arXiv:hep-ph/9710312].
 - [57] F. Borzumati and C. Greub, *2HDMs predictions for anti- $B \rightarrow X/s$ gamma in NLO (QCD)*, *Phys. Rev. D* **58** (1998) 074004, [arXiv:hep-ph/9802391].

- [58] T. M. Aliev and E. O. Iltan, *B/s \rightarrow gamma gamma decay in the two Higgs doublet model with flavour changing neutral currents*, *Phys. Rev. D* **58** (1998) 095014, [arXiv:hep-ph/9803459].
- [59] M. Misiak and M. Steinhauser, *NNLO QCD corrections to the $B \rightarrow X_s$ gamma matrix elements using interpolation in m_c* , *Nucl. Phys. B* **764** (2007) 62, [arXiv:hep-ph/0609241].
- [60] M. Misiak, H. M. Asatrian, K. Bieri, M. Czakon, A. Czarnecki, T. Ewerth, A. Ferroglia, P. Gambino, M. Gorbahn, C. Greub, U. Haisch, A. Hovhannisyan, T. Hurth, A. Mitov, V. Poghosyan, M. Slusarczyk, M. Steinhauser, *Estimate of $BR(B \rightarrow X_s \text{ gamma})$ at $O(\alpha_s^2)$* , *Phys. Rev. Lett.* **98** (2007) 022002, [arXiv:hep-ph/0609232].
- [61] T. Becher and M. Neubert, *Analysis of $Br(B \rightarrow X/s \text{ gamma})$ at NNLO with a cut on photon energy*, *Phys. Rev. Lett.* **98** (2007) 022003, [arXiv:hep-ph/0610067].
- [62] D. A. Ross and M. J. G. Veltman, *Neutral Currents In Neutrino Experiments*, *Nucl. Phys. B* **95** (1975) 135.
- [63] M. B. Einhorn, D. R. T. Jones and M. J. G. Veltman, *Heavy Particles And The Rho Parameter In The Standard Model*, *Nucl. Phys. B* **191** (1981) 146.
- [64] A. Belyaev, D. Garcia, J. Guasch and J. Sola, *Prospects for heavy supersymmetric charged Higgs boson searches at hadron colliders*, *JHEP* **0206** (2002) 059, [arXiv:hep-ph/0203031].
- [65] D. Eriksson, J. Rathsmann and O. Stal, *2HDMC: Two-Higgs-doublet model calculator*, *Comput. Phys. Commun.* **181** (2010) 833.
- [66] D. Eriksson, J. Rathsmann and O. Stal, *2HDMC - Two-Higgs-Doublet Model Calculator: Physics and Manual*, *Comput. Phys. Commun.* **181** (2010) 189, [arXiv:0902.0851, hep-ph].
- [67] N. D. Christensen and C. Duhr, *FeynRules - Feynman rules made easy*, *Comput. Phys. Commun.* **180** (2009) 1614, [arXiv:0806.4194, hep-ph].
- [68] A. Arhrib, R. Benbrik, C. H. Chen, R. Guedes and R. Santos, *Double Neutral Higgs production in the Two-Higgs doublet model at the LHC*, *JHEP* **0908** (2009) 035, [arXiv:0906.0387, hep-ph].
- [69] M. N. Dubinin, A. V. Semenov, *Triple and quartic interactions of Higgs bosons in the two-Higgs-doublet model with CP violation*, *Eur. Phys. J. C* **28** (2003) 223-236, [arXiv:hep-ph/0206205].
- [70] M. Malinsky, J. Horejsi, *Triple gauge vertices at one-loop level in THDM*, *Eur. Phys. J. C* **34** (2004) 477-486, [arXiv:hep-ph/0308247].
- [71] J. A. M. Vermaseren, *New features of FORM*, [arXiv:math-ph/0010025].